Mathematical Models and Methods in Applied Sciences
Vol. 22, No. 3 (2012) 1150015 (40 pages)

DOI: 10.1142/S0218202511500151

World Scientific
www.worldscientific.com

CERTIFIED REDUCED BASIS METHODS FOR NONAFFINE LINEAR TIME-VARYING AND NONLINEAR PARABOLIC PARTIAL DIFFERENTIAL EQUATIONS

MARTIN A. GREPL

Numerical Mathematics, RWTH Aachen University,
Templergraben 55, 52056 Aachen, Germany
grepl@igpm.rwth-aachen.de

Received 31 March 2010
Revised 12 May 2011
Communicated by F. Brezzi

We present reduced basis approximations and associated *a posteriori* error bounds for parabolic partial differential equations involving (i) a nonaffine dependence on the parameter and (ii) a nonlinear dependence on the field variable. The method employs the Empirical Interpolation Method in order to construct "affine" coefficient-function approximations of the "nonaffine" (or nonlinear) parametrized functions. We consider linear time-invariant as well as linear time-varying nonaffine functions and introduce a new sampling approach to generate the function approximation space for the latter case. Our *a posteriori* error bounds take both error contributions explicitly into account — the error introduced by the reduced basis approximation *and* the error induced by the coefficient function interpolation. We show that these bounds are rigorous upper bounds for the approximation error under certain conditions on the function interpolation, thus addressing the demand for certainty of the approximation. As regards efficiency, we develop an offline–online computational procedure for the calculation of the reduced basis approximation and associated error bound. The method is thus ideally suited for the many-query or real-time contexts. Numerical results are presented to confirm and test our approach.

Keywords: Reduced basis methods; parabolic PDEs; parameter-dependent systems; time-varying PDEs; nonlinear PDEs; nonaffine parameter dependence; *a posteriori* error estimation; Galerkin approximation.

AMS Subject Classification: 35K15, 35K55, 65M15

1. Introduction

The role of numerical simulation in engineering and science has become increasingly important. System or component behavior is often modeled using a set of partial differential equations and associated boundary conditions, the analytical solution to which is generally unavailable. In practice, a discretization procedure such as the finite element method (FEM) is used.

However, as the physical problems become more complex and the mathematical models more involved, current computational methods prove increasingly inadequate, especially in contexts requiring numerous solutions of parametrized partial differential equations for many different values of the parameter. Even for modest-complexity models, the computational cost to solve these problems is prohibitive.

For example, the design, optimization, control, and characterization of engineering components or systems often require repeated, reliable, and real-time prediction of performance metrics, or outputs, s^{e}, such as heat fluxes or flowrates.[a] These outputs are typically functionals of field variables, y^{e} — such as temperatures or velocities — associated with a parametrized partial differential equation; the parameters, or inputs, μ, serve to identify a particular configuration of the component — such as boundary conditions, material properties, and geometry. The relevant system behavior is thus described by an implicit input–output relationship, $s^{\mathrm{e}}(\mu)$, evaluation of which demands solution of the underlying partial differential equation (PDE).

Our focus here is on parabolic PDEs. For simplicity, we will directly consider a time-discrete framework associated to the time interval $I \equiv]0, t_f]$ ($\bar{I} \equiv [0, t_f]$). We divide $\bar{I}$ into K subintervals of equal length $\Delta t = \frac{t_f}{K}$ and define $t^k \equiv k\Delta t$, $0 \leq k \leq K \equiv \frac{t_f}{\Delta t}$, and $\mathbb{I} \equiv \{t^0, \ldots, t^K\}$; for notational convenience, we also introduce $\mathbb{K} \equiv \{1, \ldots, K\}$. We shall consider Euler–Backward for the time integration although higher-order schemes such as Crank–Nicolson can also be readily treated.[17] We refer to Ref. 41 for a reduced basis approach for parabolic problems using arbitrary-order Discontinuous-Galerkin temporal schemes. The abstract formulation can be stated as follows: given any $\mu \in \mathcal{D} \subset \mathbb{R}^P$, we evaluate the output $s^{\mathrm{e},k}(\mu) \equiv s^{\mathrm{e}}(t^k; \mu) = \ell(y^{\mathrm{e},k}(\mu)), \forall\, k \in \mathbb{K}$, where $y^{\mathrm{e},k}(\mu) \equiv y^{\mathrm{e}}(t^k; \mu) \in X^{\mathrm{e}}$ satisfies

$$m(y^{\mathrm{e},k}(\mu), v) + \Delta t a(y^{\mathrm{e},k}(\mu), v; \mu) = m(y^{\mathrm{e},k-1}(\mu), v) + \Delta t f(v; \mu) u(t^k), \quad \forall\, v \in X^{\mathrm{e}}, \quad \forall\, k \in \mathbb{K}, \tag{1.1}$$

with initial condition (say) $y^{\mathrm{e}}(t^0; \mu) = y_0^{\mathrm{e}}(\mu) = 0$. Here, $\mathcal{D}$ is the parameter domain in which our P-tuple (input) parameter μ resides, X^{e} is an appropriate Hilbert space, and $\Omega \subset \mathbb{R}^d$ is our spatial domain, a point in which shall be denoted x. Furthermore, $a(\cdot, \cdot; \mu)$ and $m(\cdot, \cdot)$ are X^{e}-continuous and Y^{e}-continuous ($X^{\mathrm{e}} \subset Y^{\mathrm{e}}$) bounded bilinear forms, respectively; $f(\cdot; \mu), \ell(\cdot)$ are Y^{e}-continuous bounded linear functionals; and $u(t^k)$ is the "control input" at time $t = t^k$. We assume here that $\ell(\cdot)$ and $m(\cdot, \cdot)$ do not depend on the parameter; parameter dependence, however, is readily admitted.[19]

Since the exact solution is usually unavailable, numerical solution techniques must be employed to solve (1.1). Classical approaches such as the finite element method typically cannot satisfy the requirements of *real-time certified* prediction

[a]Here superscript "e" shall refer to "exact". We shall later introduce a "truth approximation" which will bear no superscript.

of the outputs of interest. In the finite element method, the infinite-dimensional solution space is replaced by a finite-dimensional "truth" approximation space $X \subset X^{\mathrm{e}}$ of size $\mathcal{N}$: for any $\mu \in \mathcal{D}$, we evaluate the output

$$s^k(\mu) = \ell(y^k(\mu)), \quad \forall\, k \in \mathbb{K}, \tag{1.2}$$

where $y^k(\mu) \in X$ satisfies

$$m(y^k(\mu), v) + \Delta t a(y^k(\mu), v; \mu) = m(y^{k-1}(\mu), v) + \Delta t f(v; \mu) u(t^k), \quad \forall\, v \in X, \quad \forall\, k \in \mathbb{K}, \tag{1.3}$$

with initial condition $y(\mu, t^0) = y_0(\mu) = 0$. We shall assume — hence the appellation "truth" — that the approximation space is sufficiently rich such that the FEM approximation $y^k(\mu)$ (respectively, $s^k(\mu)$) is indistinguishable from the analytic, or exact, solution $y^{\mathrm{e},k}(\mu)$ (respectively, $s^{\mathrm{e},k}(\mu)$).

Unfortunately, for any reasonable error tolerance, the dimension $\mathcal{N}$ needed to satisfy this condition — even with the application of appropriate (parameter-dependent) adaptive mesh refinement strategies — is typically extremely large, and in particular much too large to satisfy the condition of real-time response or the need for numerous solutions. Our goal is the development of numerical methods that permit the *efficient* and *reliable* evaluation of this PDE-induced input–output relationship *in real-time* or *in the limit of many queries* — that is, in the design, optimization, control, and characterization contexts. To achieve this goal we pursue the reduced basis method. The reduced basis method was first introduced in the late 1970s for the nonlinear analysis of structures[1,33] and subsequently abstracted and analyzed[5,15,35,40]; see Ref. 42 for a recent review of contributions to the methodology.

The core requirement for the development of efficient offline–online computational strategies, i.e. online $\mathcal{N}$-independence, is the affine parameter dependence — e.g. the bilinear form $a(w, v; \mu)$ can be expressed as

$$a(w, v; \mu) = \sum_{q=1}^{Q} \Theta^q(\mu) a^q(w, v), \tag{1.4}$$

where the $\Theta^q(\mu) : \mathcal{D} \to \mathbb{R}$ are *parameter-dependent* functions and the $a^q(w, v)$ are *parameter-independent* bilinear forms. In the recent past, reduced basis approximations and associated *a posteriori* error estimation for linear and at most quadratically nonlinear elliptic and parabolic PDEs honoring this requirement have been successfully developed.[19,20,23,30,32,36,46,48,49]

In Ref. 18 we extended these results and developed efficient offline–online strategies for *reduced basis approximations* of nonaffine (and certain classes of nonlinear) elliptic and parabolic PDEs. Our approach is based on the Empirical Interpolation Method (EIM)[4] — a technique that recovers the efficient offline–online decomposition even in the presence of nonaffine parameter dependence. We can thus develop

an "online $\mathcal{N}$-independent" computational decomposition even for nonaffine parameter dependence, i.e. where for *general* $g(x;\mu)$ (here $x \in \Omega$ and $\mu \in \mathcal{D}$) the bilinear form satisfies

$$a(w,v;\mu) \equiv \int_\Omega \nabla w \cdot \nabla v + \int_\Omega g(x;\mu) wv. \tag{1.5}$$

A posteriori error bounds for nonaffine linear and certain classes of nonaffine nonlinear elliptic problems have been proposed in Refs. 31 and 7, respectively. In this paper, we shall consider the extension of these techniques and develop *a posteriori* error bounds (i) for nonaffine linear time-varying parabolic problems, and (ii) for problems in which g is a nonaffine *nonlinear* function of the parameter μ (possibly including time), spatial coordinate x, *and* field variable y — we hence treat certain classes of nonlinear problems. We recall that the computational cost to generate the collateral reduced basis space for the function approximation is very high in the parabolic case if the function g is time-varying either through an explicit dependence on time or an implicit dependence *via* the field variable $y(t^k;\mu)$.[18] We therefore propose a novel more efficient approach to generate the collateral reduced basis space which is based on a POD (in time)/Greedy (in parameter space) search.[20]

A large number of model order reduction (MOR) techniques[2,8,9,29,34,39,44,50] have been developed to treat (nonlinear) time-dependent problems. One approach is linearization[50] and polynomial approximation[9,34]: however, due to a lack of efficient representations of nonlinear terms and fast exponential growth (with the degree of the nonlinear approximation order) of computational complexity, these methods are quite expensive and do not address strong nonlinearities efficiently. Other approaches for highly nonlinear systems (such as piecewise-linearization) have also been proposed[39,43] but at the expense of high computational cost and little control over model accuracy. Furthermore, although *a priori* error bounds to quantify the error due to model reduction have been derived in the linear case, *a posteriori* error bounds have not yet been adequately considered even for the linear case, let alone the nonlinear case, for most MOR approaches. Finally, it is important to note that most MOR techniques focus mainly on reduced order modeling of dynamical systems in which time is considered the *only* "parameter"; the development of reduced order models for problems with a simultaneous dependence of the field variable on parameter and time — our focus here — is much less common.[6,10]

This paper is organized as follows: In Sec. 2 we first present a short review of the Empirical Interpolation Method and then extend these ideas to treat nonaffine time-varying functions. The abstract problem formulation, reduced basis approximation, associated *a posteriori* error estimation, and computational considerations for linear time-varying parabolic problems with nonaffine parameter dependence are discussed in Sec. 3. In Sec. 4, we extend these results to monotonic nonlinear parabolic PDEs. Numerical results are used throughout to test and confirm our theoretical results. We offer concluding remarks in Sec. 5.

2. Empirical Interpolation Method

The Empirical Interpolation Method, introduced in Ref. 4, serves to construct "affine" coefficient-function approximations of "nonaffine" parametrized functions. The method is frequently applied in reduced basis approximations of parametrized partial differential equations with nonaffine parameter dependence[4,18]; the affine approximation of the equations is crucial for computational efficiency. Here, we briefly summarize the results for the interpolation procedure and the estimator for the interpolation error and subsequently extend these ideas to treat nonaffine time-varying functions.

2.1. *Time-invariant parametrized functions*

2.1.1. *Coefficient-function approximation*

We are given a function $g : \Omega \times \mathcal{D} \to \mathbb{R}$ such that, for all $\mu \in \mathcal{D}$, $g(\cdot;\mu) \in L^\infty(\Omega)$. Here, $\mathcal{D} \subset \mathbb{R}^P$ is the parameter domain, $\Omega \subset \mathbb{R}^2$ is the spatial domain — a point in which shall be denoted by $x = (x_{(1)}, x_{(2)})$ — and $L^\infty(\Omega) \equiv \{v | \operatorname{ess\,sup}_{v\in\Omega} |v(x)| < \infty\}$.

We first define the nested sample sets $S_M^g \equiv \{\mu_1^g \in \mathcal{D}, \ldots, \mu_M^g \in \mathcal{D}\}$, associated reduced basis spaces $W_M^g = \operatorname{span}\{\xi_m \equiv g(x;\mu_m^g), 1 \le m \le M\}$, and nested sets of interpolation points $T_M^g = \{x_1, \ldots, x_M\}$, $1 \le M \le M_{\max}$. We present here a generalization for the construction of the EIM which allows a simultaneous definition of the generating functions W_M^g and associated interpolation points T_M^g.[28] The construction is based on a greedy algorithm[48] and is required for our POD/Greedy-EIM algorithm which we will introduce in Sec. 2.2.1.

We first choose $\mu_1^g \in \mathcal{D}$, compute $\xi_1 \equiv g(x;\mu_1^g)$, define $W_1^g \equiv \operatorname{span}\{\xi_1\}$, and set $x_1 = \arg\operatorname{ess\,sup}_{x\in\Omega} |\xi_1(x)|$, $q_1 = \xi_1(x)/\xi_1(x_1)$, and $B_{11}^1 = 1$. We then proceed by induction to generate S_M^g, W_M^g, and T_M^g: for $1 \le M \le M_{\max} - 1$, we determine $\mu_{M+1}^g \equiv \arg\max_{\mu\in\Xi_{\text{train}}^g} \|g(\cdot;\mu) - g_M(\cdot;\mu)\|_{L^\infty(\Omega)}$, compute $\xi_{M+1} \equiv g(x;\mu_{M+1}^g)$, and define $W_{M+1}^g \equiv \operatorname{span}\{\xi_m\}_{m=1}^{M+1}$. To generate the interpolation points we solve the linear system $\sum_{j=1}^M \sigma_j^M q_j(x_i) = \xi_{M+1}(x_i)$, $1 \le i \le M$ and we set $r_{M+1}(x) = \xi_{M+1}(x) - \sum_{j=1}^M \sigma_j^M q_j(x)$, $x_{M+1} = \arg\operatorname{ess\,sup}_{x\in\Omega} |r_{M+1}(x)|$, and $q_{M+1}(x) = r_{M+1}(x)/r_{M+1}(x_{M+1})$. Here, $\Xi_{\text{train}}^g \subset \mathcal{D}$ is a finite but suitably large train sample which shall serve as our $\mathcal{D}$ surrogate, and $g_M(\cdot;\mu) \in W_M^g$ is the EIM interpolant of $g(\cdot;\mu)$ over the set T_M^g for any $\mu \in \mathcal{D}$. Specifically

$$g_M(x;\mu) \equiv \sum_{m=1}^M \varphi_{Mm}(\mu) q_m, \tag{2.1}$$

where

$$\sum_{j=1}^M B_{ij}^M \varphi_{Mj}(\mu) = g(x_i;\mu), \quad 1 \le i \le M, \tag{2.2}$$

and the matrix $B^M \in \mathbb{R}^{M\times M}$ is defined such that $B_{ij}^M = q_j(x_i)$, $1 \le i, j \le M$. We note that the determination of the coefficients $\varphi_{Mm}(\mu)$ requires only $\mathcal{O}(M^2)$

computational cost since B^M is lower triangular with unity diagonal and that $\{q_m\}_{m=1}^M$ is a basis for W_M^g.[4,18]

Finally, we define a "Lebesgue constant"[37] $\Lambda_M \equiv \sup_{x\in\Omega} \sum_{m=1}^M |V_m^M(x)|$, where $V_m^M(x) \in W_M^g$ are the characteristic functions of W_M^g satisfying $V_m^M(x_n) \equiv \delta_{mn}$, $1 \le m, n \le M$; here, δ_{mn} is the Kronecker delta symbol. We recall that (i) the set of all characteristic functions $\{V_m^M\}_{m=1}^M$ is a basis for W_M^g, and (ii) the Lebesgue constant Λ_M satisfies $\Lambda_M \le 2^M - 1$.[4,18] In applications, the actual asymptotic behavior of Λ_M is much lower, as we shall observe subsequently.

2.1.2. A posteriori *error estimation*

Given an approximation $g_M(x;\mu)$ for $M \le M_{\max} - 1$, we define $\mathcal{E}_M(x;\mu) \equiv \hat{\varepsilon}_M(\mu) q_{M+1}(x)$, where $\hat{\varepsilon}_M(\mu) \equiv |g(x_{M+1};\mu) - g_M(x_{M+1};\mu)|$. We also define the interpolation error as

$$\varepsilon_M(\mu) \equiv \|g(\cdot;\mu) - g_M(\cdot;\mu)\|_{L^\infty(\Omega)}. \tag{2.3}$$

In general, $\varepsilon_M(\mu) \ge \hat{\varepsilon}_M(\mu)$, since $\varepsilon_M(\mu) \ge |g(x;\mu) - g_M(x;\mu)|$ for all $x \in \Omega$, and thus also for $x = x_{M+1}$. However, we can prove (see Refs. 4, 18 and 28)

Proposition 2.1. *If* $g(\cdot;\mu) \in W_{M+1}^g$, *then* (i) $g(x;\mu) - g_M(x;\mu) = \pm\mathcal{E}_M(x;\mu)$ (*either* $\mathcal{E}_M(x;\mu)$ *or* $-\mathcal{E}_M(x;\mu)$), *and* (ii) $\|g(\cdot;\mu) - g_M(\cdot;\mu)\|_{L^\infty(\Omega)} = \hat{\varepsilon}_M(\mu)$.

Of course, in general $g(\cdot;\mu) \notin W_{M+1}^g$, and hence our estimator $\hat{\varepsilon}_M(\mu)$ is indeed a lower bound. However, if $\varepsilon_M(\mu) \to 0$ very fast, we expect that the effectivity,

$$\eta_M(\mu) \equiv \frac{\hat{\varepsilon}_M(\mu)}{\varepsilon_M(\mu)}, \tag{2.4}$$

shall be close to unity. Furthermore, the estimator is very inexpensive — *one additional evaluation* of $g(\cdot;\mu)$ at a single point in Ω.

Finally, we note that we can readily improve the rigor of our bound by relaxing the condition $g(\cdot;\mu) \in W_{M+1}^g$. In fact, since the space W_M^g is hierarchical, i.e. $W_1^g \subset W_2^g \subset \cdots \subset W_{M_{\max}}^g$, the assumption $g(\cdot;\mu) \in W_M^g$ is more likely to hold as we increase the dimension M of the approximation space. Thus, given an approximation $g_M(x;\mu)$ for $M \le M_{\max} - k$, we can show that if $g(\cdot;\mu) \in W_{M+k}^g$, then $\tilde{\varepsilon}_M(\mu) = 2^{k-1} \max_{i\in\{1,\ldots,k\}} |g(x_{M+i};\mu) - g_M(x_{M+i};\mu)|$ is an upper bound for the interpolation error $\varepsilon_M(\mu)$.[18] This relaxation of the assumption on $g(x;\mu)$ only comes at a modest additional cost — we need to evaluate $g(\cdot;\mu)$ at k additional points in Ω.

2.1.3. *Numerical results*

We consider the function $g(\cdot;\mu) = G(\cdot;\mu)$, where

$$G(x;\mu) \equiv \frac{1}{\sqrt{(x_{(1)} - \mu_1)^2 + (x_{(2)} - \mu_2)^2}}, \tag{2.5}$$

for $x \in \Omega =]0,1[^2 \in \mathbb{R}^2$ and $\mu \in \mathcal{D} \equiv [-1,-0.01]^2$. From a physical point of view, $G(x;\mu)$ describes the gravity potential of a unit mass located at the position (μ_1,μ_2) in the spatial domain.

We introduce a triangulation of Ω with $\mathcal{N} = 2601$ vertices over which we realize $G(\cdot;\mu)$ as a piecewise linear function. We choose for $\Xi_{\text{train}} \subset \mathcal{D}$ a deterministic grid of 40×40 parameter points over $\mathcal{D}$ and we take $\mu_1^g = (-0.01,-0.01)$. Next, we pursue the empirical interpolation procedure described in Sec. 2.1.1 to construct S_M^g, W_M^g, T_M^g, and B^M, $1 \le M \le M_{\max}$, for $M_{\max} = 57$.

We now introduce a parameter test sample Ξ_{Test} of size $Q_{\text{Test}} = 225$, and define the maximum error $\varepsilon_{M,\max} = \max_{\mu\in\Xi_{\text{Test}}} \varepsilon_M(\mu)$, the maximum error estimator $\hat{\varepsilon}_{M,\max} = \max_{\mu\in\Xi_{\text{Test}}} \hat{\varepsilon}_M(\mu)$, the average effectivity $\bar{\eta}_M = Q_{\text{Test}}^{-1} \sum_{\mu\in\Xi_{\text{Test}}} \eta_M(\mu)$, where $\eta_M(\mu)$ is the effectivity defined in (2.4), and $\varkappa_M$ is the condition number of B^M. We present in Table 1 $\varepsilon_{M,\max}$, $\hat{\varepsilon}_{M,\max}$, $\bar{\eta}_M$, Λ_M, and $\varkappa_M$ as a function of M. We observe that $\varepsilon_{M,\max}$ and the bound $\hat{\varepsilon}_{M,\max}$ converge rapidly with M and that the error estimator effectivity is less than but reasonably close to unity. We also note that the Lebesgue constant grows very slowly and that B^M is quite well-conditioned for our choice of basis.

2.2. *Time-varying parametrized functions*

2.2.1. *Coefficient-function approximation*

We extend the previous results and consider parametrized nonaffine time-varying functions $g_t : \Omega \times I \times \mathcal{D} \to \mathbb{R}$. We assume that g_t is smooth in time; for simplicity here, we assume that for all $\mu \in \mathcal{D}$, $g_t(\cdot,\cdot;\mu) \in C^\infty(I, L^\infty(\Omega))$. Note that we use the subscript t to signify the dependence on time. We consider the time-discretization introduced in Sec. 1 and — analogous to the notation used for the field variable $y^k(\mu)$ — write $g_t^k(x;\mu) = g_t(x,t^k;\mu)$.

We first consider the construction of the nested sample sets $S_M^{g_t}$, associated reduced basis spaces $W_M^{g_t}$, and nested sets of interpolation points $T_M^{g_t}$. To this end, we propose a new POD/Greedy-EIM procedure which combines the greedy selection procedure in parameter space, described in Sec. 2.1.1 for nonaffine time-invariant functions, with the Proper Orthogonal Decomposition (POD) in time.

Table 1. Numerical results for empirical interpolation of $G(x;\mu)$: $\varepsilon_{M,\max}, \hat{\varepsilon}_{M,\max}, \bar{\eta}_M, \Lambda_M$, and $\varkappa_M$ as a function of M.

M	$\varepsilon_{M,\max}$	$\hat{\varepsilon}_{M,\max}$	$\bar{\eta}_M$	Λ_M	$\varkappa_M$
8	2.05E−01	1.62E−01	0.17	1.98	3.73
16	8.54E−03	8.54E−03	0.85	2.26	6.01
24	6.53E−04	6.49E−04	0.50	3.95	8.66
32	1.29E−04	1.28E−05	0.73	5.21	12.6
40	1.37E−05	1.35E−06	0.43	5.18	16.6
48	4.76E−06	1.78E−07	0.19	10.2	20.0

Let $\text{POD}_Y(\{g_t^k(\cdot;\mu), 1 \le k \le K\}, R)$ return the R largest POD modes, $\{\chi_i, 1 \le i \le R\}$, with respect to the $(\cdot,\cdot)_Y$ inner product. We recall that the POD modes, χ_i, are mutually Y-orthogonal such that $\mathcal{P}_R = \text{span}\{\chi_i, 1 \le i \le R\}$ satisfies the optimality property

$$\mathcal{P}_R = \arg \inf_{Y_R \subset \text{span}\{g_t^k(\cdot;\mu), 1 \le k \le K\}} \left(\frac{1}{K} \sum_{k=1}^{K} \inf_{w \in Y_R} \|g_t^k(\cdot;\mu) - w\|_Y^2 \right), \tag{2.6}$$

where Y_R denotes a linear space of dimension R. Here, we are only interested in the largest POD mode which we obtain using the method of snapshots.[44] To this end, we solve the eigenvalue problem $C\psi^i = \lambda^i \psi^i$ for $(\psi^1 \in \mathbb{R}^K, \lambda^1 \in \mathbb{R})$ associated with the largest eigenvalue of C, where $C_{ij} = (g_t^i(\cdot;\mu), g_t^j(\cdot;\mu))_Y, 1 \le i, j \le K$. We then obtain the first POD mode from $\chi_1 = \sum_{k=1}^K \psi_k^1 g_t^k(\cdot;\mu)$.

Before summarizing the POD/Greedy-EIM procedure, we define the EIM interpolant in the time-varying case as

$$g_{t,M}^k(x;\mu) \equiv \sum_{m=1}^{M} \varphi_{Mm}^k(\mu) q_m, \quad \forall\, k \in \mathbb{K}, \tag{2.7}$$

where

$$\sum_{j=1}^{M} B_{ij}^M \varphi_{Mj}^k(\mu) = g_t^k(x_i;\mu), \quad 1 \le i \le M, \ \forall\, k \in \mathbb{K}. \tag{2.8}$$

We note that the computational cost to determine the time-varying coefficients $\varphi_{Mm}^k(\mu), 1 \le m \le M$, for all timesteps is $\mathcal{O}(KM^2)$. The POD/Greedy-EIM procedure is summarized in Algorithm 1.

2.2.2. A posteriori *error estimation*

The *a posteriori* error estimation procedure for the time-varying case directly follows from the time-invariant case of Sec. 2.1.2. We first define the time-varying interpolation error as

$$\varepsilon_{t,M}^k(\mu) \equiv \|g_t^k(x;\mu) - g_{t,M}^k(x;\mu)\|_{L^\infty(\Omega)}, \quad \forall\, k \in \mathbb{K}, \tag{2.9}$$

and the estimator $\hat{\varepsilon}_{t,M}^k(\mu) \equiv |g_t^k(x_{M+1};\mu) - g_{t,M}^k(x_{M+1};\mu)|, \forall\, k \in \mathbb{K}$. The estimator for the interpolation error at each timestep follows from Proposition 2.1 and is stated in

Corollary 2.1. *If* $g_t^k(\cdot;\mu) \in W_{M+1}^{g_t}$ *for all* $k \in \mathbb{K}$, *then* (i) $g_t^k(x;\mu) - g_{t,M}^k(x;\mu) = \pm\hat{\varepsilon}_{t,M}^k(\mu) q_{M+1}(x), \forall\, k \in \mathbb{K}$, *and* (ii) $\|g_t^k(\cdot;\mu) - g_{t,M}^k(\cdot;\mu)\|_{L^\infty(\Omega)} = \hat{\varepsilon}_{t,M}^k(\mu), \forall\, k \in \mathbb{K}$.

We note that the condition $g_t^k(\cdot;\mu) \in W_{M+1}^{g_t}$ has to hold for all timesteps and is thus more restrictive than in the time-invariant case. In general, $\hat{\varepsilon}_{t,M}^k(\mu)$ is a lower

Algorithm 1. POD/Greedy-EIM Algorithm

specify $\Xi^g_{\text{train}} \subset \mathcal{D}$, $M_{\max}$, $\mu_1^{g_t} \in \mathcal{D}$ (arbitrary).
$\xi_1 \equiv \text{POD}_Y(\{g_t^k(\cdot;\mu_1^{g_t}), 1 \le k \le K\}, 1)$.
set $M = 1$, $S_1^{g_1} = \{\mu_1^{g_t}\}$, $W_1^{g_t} \equiv \text{span}\{\xi_1\}$.
set $x_1 = \arg\operatorname{ess\,sup}_{x\in\Omega} |\xi_1(x)|$, $q_1 = \xi_1(x)/\xi_1(x_1)$, and $B_{11}^1 = 1$.
while $M \le M_{\max} - 1$ **do**
  $\mu_{M+1}^{g_t} = \arg\max_{\mu\in\Xi_{\text{train}}} \Delta t \sum_{k=1}^K \|g_t^k(\cdot;\mu) - g_{t,M}^k(\cdot;\mu)\|_{L^\infty(\Omega)}$,
    where $g_{t,M}^k$ is calculated from (2.7) and (2.8);
  $e_{M,\text{EIM}}^k(\mu) = g_t^k(x;\mu_{M+1}^{g_t}) - g_{t,M}^k(x;\mu_{M+1}^{g_t})$, $1 \le k \le K$;
  $\xi_{M+1} = \text{POD}_Y(\{e_{M,\text{EIM}}^k(\mu_{M+1}^{g_t}), 1 \le k \le K\}, 1)$;
  $W_{M+1}^{g_t} \leftarrow W_M^{g_t} \oplus \text{span}\{\xi_{M+1}\}$;
  $S_{M+1}^{g_t} \leftarrow S_M^{g_t} \cup \mu_{M+1}^{g_t}$;
  solve for σ_j^M from $\sum_{j=1}^M \sigma_j^M q_j(x_i) = \xi_{M+1}(x_i)$, $1 \le i \le M$;
  set $r_{M+1}(x) = \xi_{M+1}(x) - \sum_{j=1}^M \sigma_j^M q_j(x)$;
  set $x_{M+1} = \arg\operatorname{ess\,sup}_{x\in\Omega} |r_{M+1}(x)|$;
  set $q_{M+1}(x) = r_{M+1}(x)/r_{M+1}(x_{M+1})$;
  update $B_{ij}^{M+1} = q_j(x_i)$, $1 \le i, j \le M+1$;
  $M \leftarrow M + 1$;
end

bound for the interpolation error at each timestep. Finally, we may also define the effectivity

$$\eta_{t,M}^k(\mu) \equiv \frac{\hat{\varepsilon}_{t,M}^k(\mu)}{\varepsilon_{t,M}^k(\mu)}, \quad \forall\, k \in \mathbb{K}. \tag{2.10}$$

Again, our estimator is very inexpensive — at each individual timestep we have to perform only *one additional evaluation* of $g_t^k(\cdot;\mu)$ at a single point in Ω.

2.2.3. *Numerical results*

We consider the nonaffine time-varying function $g_t^k(\cdot;\mu) = G_t^k(\cdot;\mu)$, where

$$G_t^k(x;\mu) \equiv \frac{1}{\sqrt{(x_{(1)} - (\mu_1 - t^k/2))^2 + (x_{(2)} - (\mu_2 - t^k/2))^2}}, \tag{2.11}$$

for $x \in \Omega =]0,1[^2 \in \mathbb{R}^2$, $t^k \in \mathbb{I}$, and $\mu \in \mathcal{D} \equiv [-1, -0.01]^2$. Compared to the stationary problem (2.5), $G_t(x;\mu)$ describes the gravity potential of a unit mass

which is now moving in the spatial domain, i.e. the mass is initially located at the position (μ_1, μ_2) and then moving with velocity $(-1/2, -1/2)$ as time proceeds.

We use the triangulation of Ω and Ξ_{train} from Sec. 2.1.3 and take $\mu_1^{g_t} = (-0.01, -0.01)$. Next, we employ Algorithm 1 to construct $S_M^{g_t}$, $W_M^{g_t}$, $T_M^{g_t}$, and B^M, $1 \leq M \leq M_{\max}$, for $M_{\max} = 49$. We define the maximum error $\varepsilon_{t,M,\max} = \max_{\mu\in\Xi_{\text{Test}}} \max_{k\in\mathbb{K}} \varepsilon_{t,M}^k(\mu)$, maximum error bound $\hat{\varepsilon}_{t,M,\max} = \max_{\mu\in\Xi_{\text{Test}}} \max_{k\in\mathbb{K}} \hat{\varepsilon}_{t,M}^k(\mu)$, and the average effectivity $\bar{\eta}_{t,M} = (KQ_{\text{Test}})^{-1} \sum_{\mu\in\Xi_{\text{Test}}} \sum_{k\in\mathbb{K}} \eta_{t,M}^k(\mu)$. Here, we use the parameter test sample Ξ_{Test} of size $Q_{\text{Test}} = 225$ from Sec. 2.1.3.

We present in Table 2 $\varepsilon_{t,M,\max}$, $\hat{\varepsilon}_{t,M,\max}$, $\bar{\eta}_{t,M}$, the Lebesgue constant Λ_M, and the condition number of B^M, $\varkappa_M$, as a function of M. Similar to the time-invariant case, the maximum error and bound converge rapidly with M and the error estimator effectivity is less than but still reasonably close to unity. However, $\varepsilon_{t,M,\max}$ and $\hat{\varepsilon}_{t,M,\max}$ are always larger than the corresponding time-invariant quantities in Table 1 for the same value of M. This is to be expected since time acts like an additional, albeit special, parameter. In fact, for the numerical example considered here, the time dependence effectively increases the admissible parameter domain $\mathcal{D}$ of the time-invariant problem. Finally, we note that the Lebesgue constant grows very slowly and that B^M remains well-conditioned also for the time-varying case.

3. Nonaffine Linear Time-Varying Parabolic Equations

In this section we consider reduced basis approximations and associated *a posteriori* error estimation procedures for linear parabolic PDEs with nonaffine parameter dependence. We derive the theoretical results for linear time-varying (LTV) problems and occasionally comment on the simplifications that arise for linear time-invariant (LTI) problems. Numerical results are presented for both the LTI and LTV problem.

3.1. *Problem statement*

3.1.1. *Abstract formulation*

We first recall the Hilbert spaces $X^{\text{e}} \equiv H_0^1(\Omega)$ — or, more generally, $H_0^1(\Omega) \subset X^{\text{e}} \subset H^1(\Omega)$ — and $Y^{\text{e}} \equiv L^2(\Omega)$, where $H^1(\Omega) \equiv \{v | v \in L^2(\Omega), \nabla v \in (L^2(\Omega))^d\}$, $H_0^1(\Omega) \equiv \{v | v \in H^1(\Omega), v|_{\partial\Omega} = 0\}$, and $L^2(\Omega)$ is the space of square integrable

Table 2. Numerical results for empirical interpolation of $G_t^k(x;\mu)$, $1 \leq k \leq K$: $\varepsilon_{t,M,\max}$, $\hat{\varepsilon}_{t,M,\max}$, $\bar{\eta}_{t,M}$, Λ_M, and $\varkappa_M$ as a function of M.

M	$\varepsilon_{t,M,\max}$	$\hat{\varepsilon}_{t,M,\max}$	$\bar{\eta}_{t,M}$	Λ_M	$\varkappa_M$
8	4.79E−01	4.79E−01	0.58	3.67	6.26
16	2.76E−02	2.39E−02	0.56	5.11	13.0
24	3.09E−03	3.09E−03	0.77	6.47	18.8
32	1.99E−04	1.15E−04	0.60	11.4	27.7
40	9.13E−05	9.13E−05	0.34	8.84	45.8
48	1.11E−05	5.16E−06	0.11	9.05	54.4

functions over Ω.[38] Here Ω is a bounded domain in $\mathbb{R}^d$ with Lipschitz continuous boundary $\partial\Omega$. The inner product and norm associated with $X^{\mathrm{e}}(Y^{\mathrm{e}})$ are given by $(\cdot,\cdot)_{X^{\mathrm{e}}}$ ($(\cdot,\cdot)_{Y^{\mathrm{e}}}$) and $\|\cdot\|_{X^{\mathrm{e}}} = (\cdot,\cdot)_{X^{\mathrm{e}}}^{1/2}$ ($\|\cdot\|_{Y^{\mathrm{e}}} = (\cdot,\cdot)_{Y^{\mathrm{e}}}^{1/2}$), respectively; for example, $(w,v)_{X^{\mathrm{e}}} \equiv \int_\Omega \nabla w\cdot\nabla v + \int_\Omega wv, \forall\, w,v \in X^{\mathrm{e}}$, and $(w,v)_{Y^{\mathrm{e}}} \equiv \int_\Omega wv, \forall\, w,v \in Y^{\mathrm{e}}$. The truth approximation subspace $X \subset X^{\mathrm{e}} (\subset Y^{\mathrm{e}})$ shall inherit this inner product and norm: $(\cdot;\cdot)_X \equiv (\cdot;\cdot)_X^{\mathrm{e}}$ and $\|\cdot\|_X \equiv \|\cdot\|_X^{\mathrm{e}}$; we further define $Y \equiv Y^{\mathrm{e}}$.

We directly consider the truth approximation statement defined in (1.3) with the output given by (1.2), where the bilinear form a is given by

$$a_t^k(w,v;\mu) = a_0(w,v) + a_1(w,v,g_t^k(x;\mu)), \quad \forall\, k \in \mathbb{K}, \tag{3.1}$$

and

$$f(v;g_t^k(x;\mu)) = \int_\Omega v g_t^k(x;\mu), \quad \forall\, k \in \mathbb{K}. \tag{3.2}$$

Here, $a_0(\cdot,\cdot)$ is a continuous (and, for simplicity, parameter-independent) bilinear form and $a_1 : X \times X \times L^\infty(\Omega)$ is a trilinear form. We shall use the subscript "t" notation to signify the dependence of the bilinear form a_t^k on time. We obtain the LTI problem simply by replacing $g_t^k(x;\mu)$ with the nonaffine time-invariant function $g(x;\mu)$ in (3.1) and (3.2).

We shall further assume that $a_t^k(\cdot,\cdot;\mu)$, $\forall\, k \in \mathbb{K}$, and $m(\cdot,\cdot)$ are continuous

$$a_t^k(w,v;\mu) \le \gamma_a(\mu)\|w\|_X\|v\|_X \le \gamma_a^0\|w\|_X\|v\|_X, \quad \forall\, w,v \in X, \ \forall\, \mu \in \mathcal{D}, \tag{3.3}$$

$$m(w,v) \le \gamma_m^0\|w\|_Y\|v\|_Y, \quad \forall\, w,v \in X; \tag{3.4}$$

coercive,

$$0 < \alpha_a^0 \le \alpha_a(\mu) \equiv \inf_{w\in X} \frac{a_t^k(w,w;\mu)}{\|w\|_X^2}, \quad \forall\, \mu \in \mathcal{D}, \tag{3.5}$$

$$0 < \alpha_m^0 \equiv \inf_{v\in X} \frac{m(v,v)}{\|v\|_Y^2}; \tag{3.6}$$

and symmetric, $a_t^k(v,w;\mu) = a_t^k(w,v;\mu)$, $\forall\, w,v \in X$, $\forall\, \mu \in \mathcal{D}$, and $m(v,w) = m(w,v)$, $\forall\, w,v \in X$, $\forall\, \mu \in \mathcal{D}$. (We (plausibly) suppose that γ_a^0, γ_m^0, α_a^0, α_m^0 may be chosen independent of $\mathcal{N}$.) We also assume that the trilinear form a_1 satisfies

$$a_1(w,v,z) \le \gamma_{a_1}^0\|w\|_X\|v\|_X\|z\|_{L^\infty(\Omega)}, \quad \forall\, w,v \in X, \quad \forall\, z \in L^\infty(\Omega). \tag{3.7}$$

Next, we require that the linear forms $f(\cdot;g_t^k(x;\mu)) : X \to \mathbb{R}$, $\forall\, k \in \mathbb{K}$, and $\ell(\cdot) : X \to \mathbb{R}$ be bounded with respect to $\|\cdot\|_Y$. It follows that a solution to (1.3) exists and is unique[16,45]; also see Ref. 38 for the LTI case.

3.1.2. *Model problem*

As a numerical test case for the LTI and LTV problem we consider the following nonaffine diffusion problem defined on the unit square, $\Omega =]0,1[^2 \in \mathbb{R}^2$: Given $\mu \equiv (\mu_1, \mu_2) \in \mathcal{D} \equiv [-1, -0.01]^2 \subset \mathbb{R}^{P=2}$, we evaluate $y^k(\mu) \in X$ from (1.3), where $X \subset X^e \equiv H_0^1(\Omega)$ is a linear finite element truth approximation subspace of dimension $\mathcal{N} = 2601$,

$$\begin{aligned} m(w,v) &\equiv \int_\Omega wv, \qquad a_0(w,v) \equiv \int_\Omega \nabla w \cdot \nabla v, \\ a_1(w,v,z) &\equiv \int_\Omega zwv, \qquad f(v;z) \equiv \int_\Omega zv, \end{aligned} \tag{3.8}$$

and z is given by $G(x;\mu)$ defined in (2.5) for the LTI problem and by $G_t^k(x;\mu)$ defined in (2.11) for the LTV problem. The output can be written in the form (1.2), $s^k(\mu) = \ell(y^k(\mu))$, $\forall\, k \in \mathbb{K}$, where $\ell(v) \equiv |\Omega|^{-1} \int_\Omega v$ — clearly a very smooth functional. We shall consider the time interval $\bar{I} = [0, 2]$ and a timestep $\Delta t = 0.01$; we thus have $K = 200$. We also presume the periodic control input $u(t^k) = \sin(2\pi t^k)$, $t^k \in \mathbb{I}$.

We first present results for the LTI problem (note that this problem is similar to the one used in Ref. 18). Two snapshots of the solution $y^k(\mu)$ at time $t^k = 25\Delta t$ are shown in Figs. 1(a) and 1(b) for $\mu = (-1, -1)$ and $\mu = (-0.01, -0.01)$, respectively. The solution oscillates in time and the peak is offset towards $x = (0, 0)$ for μ near the "corner" $(-0.01, -0.01)$. In Fig. 2 we plot the output $s^k(\mu)$ as a function of time for these two parameter values.

We next turn to the LTV problem and present the output $s^k(\mu)$ for $\mu = (-0.01, -0.01)$ also in Fig. 2 (dashed line). The LTV output shows a transition in time from the LTI output for $\mu = (-0.01, -0.01)$ to the LTI output for

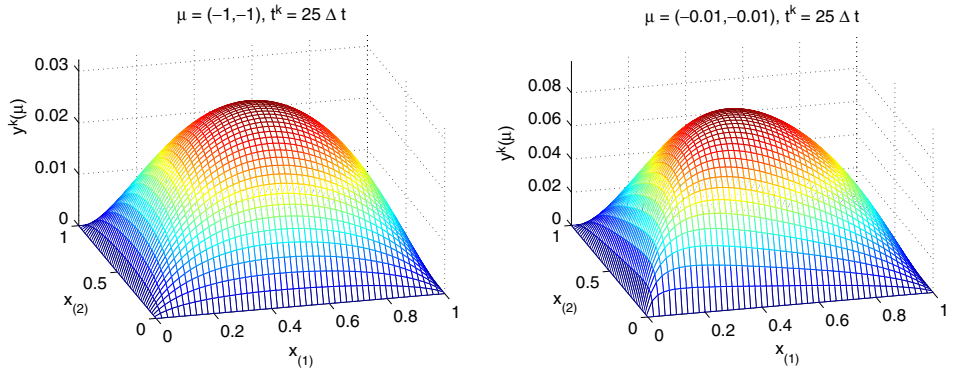

(a) (b)

Fig. 1. Solution $y^k(\mu)$ of LTI problem at $t^k = 25\Delta t$ for (a) $\mu = (-1, -1)$ and (b) $\mu = (-0.01, -0.01)$.

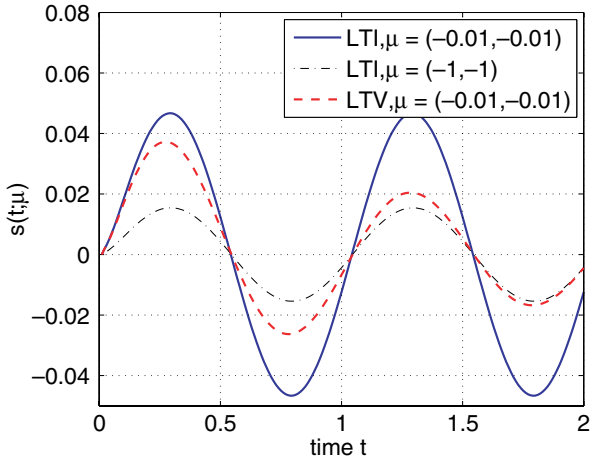

Fig. 2. Output $s^k(\mu)$ of the LTI problem for $\mu = (-0.01, -0.01)$ and $\mu = (-1, -1)$, and output of the LTV problem for $\mu = (-0.01, -0.01)$.

$\mu = (-1, -1)$. This behavior is plausible by comparing the definitions of the non-affine functions $G(x;\mu)$ and $G_t^k(x;\mu)$.

3.2. *Reduced basis approximation*

3.2.1. *Formulation*

We assume that we are given the nested Lagrangian[35] reduced basis spaces

$$W_N^y = \text{span}\{\zeta_n, 1 \le n \le N\}, \quad 1 \le N \le N_{\max}, \tag{3.9}$$

where the $\zeta_n, 1 \le n \le N$, are mutually $(\cdot,\cdot)_X$-orthogonal basis functions. We comment on the POD/Greedy algorithm for constructing the basis functions in Sec. 3.4.

Our reduced basis approximation $y_{N,M}^k(\mu)$ to $y^k(\mu)$ is then: given $\mu \in \mathcal{D}$, $y_{N,M}^k(\mu) \in W_N^y, \forall\, k \in \mathbb{K}$, satisfies

$$\begin{aligned} &m(y_{N,M}^k(\mu), v) + \Delta t(a_0(y_{N,M}^k(\mu), v) + a_1(y_{N,M}^k(\mu), v; g_{t,M}^k(x;\mu))) \\ &\quad = m(y_{N,M}^{k-1}(\mu), v) + \Delta t f(v; g_{t,M}^k(x;\mu))u(t^k), \quad \forall\, v \in W_N^y, \end{aligned} \tag{3.10}$$

with initial condition $y_{N,M}^0(\mu) = 0$. We then evaluate the output estimate, $s_{N,M}^k(\mu), \forall\, k \in \mathbb{K}$, from

$$s_{N,M}^k(\mu) \equiv \ell(y_{N,M}^k(\mu)). \tag{3.11}$$

Note that we directly replaced $g_t^k(x;\mu)$ in (3.1) by its affine approximation $g_{t,M}^k(x;\mu)$ defined in (2.7).

We now express $y^k_{N,M}(\mu) = \sum_{n=1}^N y^k_{N,Mn}(\mu)\zeta_n$, choose as test functions $v = \zeta_j$, $1 \le j \le N$, and invoke (2.7) to obtain

$$\sum_{i=1}^N \left\{ m(\zeta_i,\zeta_j) + \Delta t \left(a_0(\zeta_i,\zeta_j) + \sum_{m=1}^M \varphi^k_{Mm}(\mu) a_1(\zeta_i,\zeta_j,q_m) \right) \right\} y^k_{N,Mi}(\mu)$$
$$= \sum_{i=1}^N m(\zeta_i,\zeta_j) y^{k-1}_{N,Mi}(\mu) + \Delta t \sum_{m=1}^M \varphi^k_{Mm}(\mu) f(\zeta_j;q_m) u(t^k), \quad 1 \le j \le N, \qquad (3.12)$$

where $\varphi^k_{Mm}(\mu)$, $1 \le m \le M$, $1 \le k \le K$, is determined from (2.8). We note that (3.12) is well-posed if M is large enough such that the interpolation error satisfies $\varepsilon^k_{t,M}(\mu) \le \alpha_a(\mu)/\gamma^0_{a_1}, \forall\, k \in \mathbb{K}$. This condition on the interpolation error directly follows from (3.5) and (3.7). We can thus recover online $\mathcal{N}$-independence even for nonaffine problems: the quantities $m(\zeta_i,\zeta_j)$, $a_0(\zeta_i,\zeta_j)$, $a_1(\zeta_i,\zeta_j,q_m)$, and $f(\zeta_i;q_m)$ are all *parameter-independent* and can thus be pre-computed offline, as discussed in the next section.

3.2.2. *Computational procedure*

We summarize here the offline–online procedure.[3,22,27,36] We first express $y^k_{N,M}(\mu)$ as

$$y^k_{N,M}(\mu) = \sum_{n=1}^N y^k_{N,Mn}(\mu)\zeta_n, \qquad (3.13)$$

and choose as test functions $v = \zeta_j$, $1 \le j \le N$ in (3.10). It then follows from (3.12) that $\underline{y}^k_{N,M}(\mu) = [y^k_{N,M1}(\mu)\, y^k_{N,M2}(\mu) \cdots y^k_{N,MN}(\mu)]^T \in \mathbb{R}^N$ satisfies

$$(M_N + \Delta t A^k_N(\mu))\underline{y}^k_{N,M}(\mu) = M_N\, \underline{y}^{k-1}_{N,M}(\mu) + \Delta t F^k_N(\mu) u(t^k), \quad \forall\, k \in \mathbb{K}, \qquad (3.14)$$

with initial condition $y_{N,Mn}(\mu,t^0) = 0$, $1 \le n \le N$. Given $\underline{y}^k_{N,M}(\mu), \forall\, k \in \mathbb{K}$, we finally evaluate the output estimate from

$$s^k_{N,M}(\mu) = L^T_N \underline{y}^k_{N,M}(\mu), \quad \forall\, k \in \mathbb{K}. \qquad (3.15)$$

Here, $M_N \in \mathbb{R}^{N\times N}$ is a *parameter-independent* SPD matrix with entries

$$M_{Ni,j} = m(\zeta_j,\zeta_i), \quad 1 \le i,j \le N. \qquad (3.16)$$

Furthermore, we obtain from (2.7) and (3.1) that $A^k_N(\mu) \in \mathbb{R}^{N\times N}$ and $F^k_N(\mu) \in \mathbb{R}^N$ can be expressed as

$$A^k_N(\mu) = A_{0,N} + \sum_{m=1}^M \varphi^k_{Mm}(\mu) A^m_{1,N}, \qquad (3.17)$$

$$F^k_N(\mu) = \sum_{m=1}^M \varphi^k_{Mm}(\mu) F^m_N, \qquad (3.18)$$

where $\varphi^k_{Mm}(\mu)$, $1 \le m \le M$, is calculated from (2.8) at each timestep, and the *parameter-independent* quantities $A_{0,N} \in \mathbb{R}^{N\times N}$, $A^m_{1,N} \in \mathbb{R}^{N\times N}$, and $F^m_N \in \mathbb{R}^N$ are given by

$$\begin{aligned} A_{0,Ni,j} &= a_0(\zeta_j, \zeta_i), && 1 \le i,j \le N, \\ A^m_{1,Ni,j} &= a_1(\zeta_j, \zeta_i, q_m), && 1 \le i,j \le N,\ 1 \le m \le M, \\ F^m_{Nj} &= f(\zeta_j; q_m), && 1 \le j \le N,\ 1 \le m \le M, \end{aligned} \tag{3.19}$$

respectively. Finally, $L_N \in \mathbb{R}^N$ is the output vector with entries $L_{Ni} = \ell(\zeta_i)$, $1 \le i \le N$. We note that these quantities must be computed in a stable fashion which is consistent with the finite element quadrature points (see Ref. 17, p. 132).

The offline–online decomposition is now clear. In the offline stage — performed only *once* — we first construct the nested approximation spaces $W^{g_t}_M$ and sets of interpolation points $T^{g_t}_M$, $1 \le M \le M_{\max}$. We then solve for the ζ_n, $1 \le n \le N_{\max}$ and compute and store the μ-independent quantities in (3.16), (3.19) and L_N. The computational cost — without taking into account the construction of $W^{g_t}_M$ and $T^{g_t}_M$ — is therefore $O(KN_{\max})$ solutions of the underlying $\mathcal{N}$-dimensional "truth" finite element approximation and $O(M_{\max}N^2_{\max})$ $\mathcal{N}$-inner products; the storage requirements are also $O(M_{\max}N^2_{\max})$. In the online stage — performed many times, for each new parameter value μ — we compute $\varphi^k_{Mm}(\mu), 1 \le m \le M$, from (2.8) at cost $O(M^2)$ per timestep by multiplying the pre-computed inverse of B^M with the vector $g^k_t(x_m;\mu), 1 \le m \le M$. We then assemble the reduced basis matrix (3.17) and vector (3.18); this requires $O(MN^2)$ operations per timestep. We then solve (3.14) for $\underline{y}^k_{N,M}(\mu)$; since the reduced basis matrices are in general full, the operation count is $O(N^3)$ per timestep. The total cost to evaluate $\underline{y}^k_{N,M}(\mu)$, $\forall\, k \in \mathbb{K}$, is thus $O(K(M^2 + MN^2 + N^3))$. Finally, given $\underline{y}^k_{N,M}(\mu)$ we evaluate the output estimate $s^k_{N,M}(\mu)$, $\forall\, k \in \mathbb{K}$, from (3.15) at a cost of $O(KN)$.

Concerning the LTI problem, we note that the overall cost to evaluate $\underline{y}^k_{N,M}(\mu)$, $\forall\, k \in \mathbb{K}$, in the online stage reduces to $O(M^2 + MN^2 + N^3 + KN^2)$. We need to evaluate the time-independent coefficients $\varphi_{Mm}(\mu), 1 \le m \le M$, from (2.2) and subsequently assemble the reduced basis matrices *only once*, we may then use LU decomposition for the time stepping.

Hence, as required in the many-query or real-time contexts, the online complexity is *independent* of $\mathcal{N}$, the dimension of the underlying "truth" finite element approximation space. Since N, $M \ll \mathcal{N}$, we expect significant computational savings in the online stage relative to classical discretization and solution approaches.

3.3. A posteriori *error estimation*

We will now develop *a posteriori* error estimators which will help us to (i) assess the error introduced by our reduced basis approximation (relative to the "truth" finite element approximation); and (ii) devise an efficient procedure for generating the reduced basis space W^y_N. We recall that *a posteriori* error estimates have been

developed for reduced basis approximations of linear *affine* parabolic problems using a finite element truth discretization in Ref. 19. Subsequently, extensions to finite volume discretizations including bounds for the error in the $L^2(\Omega)$-norm have also been considered.[20]

3.3.1. *Preliminaries*

To begin, we specify the inner products $(v, w)_X \equiv a_0(v, w)$, $\forall\, v, w \in X$ and $(v, w)_Y \equiv m(v, w)$, $\forall\, v, w \in X$. We next assume that we are given a positive lower bound for the coercivity constant $\alpha_a(\mu)$: $\hat{\alpha}_a(\mu) : \mathcal{D} \to \mathbb{R}_+$ satisfies

$$\alpha_a(\mu) \geq \hat{\alpha}_a(\mu) \geq \hat{\alpha}_a^0 > 0, \quad \forall\, \mu \in \mathcal{D}. \tag{3.20}$$

We note that if $g_t^k(x; \mu) > 0, \forall\, k \in \mathbb{K}$, we may readily use $\hat{\alpha}_a(\mu) = 1$ as a lower bound. In general, however, we may need to develop a lower bound, $\hat{\alpha}_{a_1,M}(\mu)$ for the coercivity constant of the perturbed weak form $a_1(\cdot, \cdot; g_{t,M}^k(x; \mu))$ using the Successive Constraint Method (SCM).[21] In this case we directly obtain from (3.1), (3.5) and (3.7) the additional requirement that the interpolation error has to satisfy $\varepsilon_{t,M}^k(\mu) < (1 + \hat{\alpha}_{a_1,M}(\mu))/\gamma_{a_1}^0$. In some instances, simpler recipes may also suffice.[36,49]

We next introduce the dual norm of the residual

$$\varepsilon_{N,M}^k(\mu) \equiv \sup_{v \in X} \frac{R^k(v; \mu)}{\|v\|_X}, \quad \forall\, k \in \mathbb{K}, \tag{3.21}$$

where

$$R^k(v; \mu) \equiv f(v; g_{t,M}^k(x; \mu))u(t^k) - a_0(y_{N,M}^k(\mu), v) - a_1(y_{N,M}^k(\mu), v, g_{t,M}^k(x; \mu)) - \frac{1}{\Delta t} m(y_{N,M}^k(\mu) - y_{N,M}^{k-1}(\mu), v), \quad \forall\, v \in X,\ \forall\, k \in \mathbb{K}. \tag{3.22}$$

We also introduce the dual norm

$$\Phi_M^{\mathrm{na},k}(\mu) \equiv \sup_{v \in X} \frac{f(v; q_{M+1})u(t^k) - a_1(y_{N,M}^k(\mu), v, q_{M+1})}{\|v\|_X}, \quad \forall\, k \in \mathbb{K}, \tag{3.23}$$

which reflects the contribution of the nonaffine terms. Finally, we define the "spatio-temporal" energy norm, $|||v^k(\mu)|||^2 \equiv m(v^k(\mu), v^k(\mu)) + \sum_{k'=1}^k a_t^{k'}(v^{k'}(\mu), v^{k'}(\mu); \mu)\Delta t$, $\forall\, k \in \mathbb{K}$.

3.3.2. *Error bound formulation*

We obtain the following result for the error bound.

Proposition 3.1. *Suppose that $g_t^k(x; \mu) \in W_{M+1}^{g_t}$ for $1 \leq k \leq K$. The error, $e^k(\mu) \equiv y^k(\mu) - y_{N,M}^k(\mu)$, is then bounded by*

$$|||e^k(\mu)||| \leq \Delta_{N,M}^{y,k}(\mu), \quad \forall\, \mu \in \mathcal{D},\ \forall\, k \in \mathbb{K}, \tag{3.24}$$

where the error bound $\Delta_{N,M}^{y,k}(\mu) \equiv \Delta_{N,M}^{y}(t^k;\mu)$ *is defined as*

$$\Delta_{N,M}^{y,k}(\mu) \equiv \left(\frac{2\Delta t}{\hat{\alpha}_a(\mu)} \sum_{k'=1}^{k} \varepsilon_{N,M}^{k'}(\mu)^2 + \frac{2\Delta t}{\hat{\alpha}_a(\mu)} \sum_{k'=1}^{k} (\hat{\varepsilon}_{t,M}^{k'}(\mu)\Phi_M^{\mathrm{na},k'}(\mu))^2 \right)^{\frac{1}{2}}. \quad (3.25)$$

Proof. The proof is an extension of the result in Ref. 19. We thus focus on the new bits — the nonaffine parameter dependence. Following the steps in Ref. 19, we obtain

$$\begin{aligned} & m(e^k(\mu), e^k(\mu)) - m(e^{k-1}(\mu), e^{k-1}(\mu)) + \Delta t a_t^k(e^k(\mu), e^k(\mu);\mu) \\ & \quad \le \Delta t \varepsilon_{N,M}^k(\mu)\|e^k(\mu)\|_X + \Delta t\big(f(e^k(\mu); g_t^k(x;\mu) - g_{t,M}^k(x;\mu))u(t^k) \\ & \qquad - a_1(y_{N,M}^k(\mu), e^k(\mu), g_t^k(x;\mu) - g_{t,M}^k(x;\mu))\big). \end{aligned} \quad (3.26)$$

Using Young's inequality, the first term on the right-hand side can be bound by

$$2\varepsilon_N^k(\mu)\|e^k(\mu)\|_X \le \frac{2}{\hat{\alpha}_a(\mu)}\varepsilon_{N,M}^k(\mu)^2 + \frac{\hat{\alpha}_a(\mu)}{2}\|e^k(\mu)\|_X^2. \quad (3.27)$$

From our assumption, $g_t^k(x;\mu) \in W_{M+1}^{g_t}$ for $1 \le k \le K$, Corollary 2.1, and (3.23) it directly follows that

$$\begin{aligned} & f(e^k(\mu); g_t^k(x;\mu) - g_{t,M}^k(x;\mu))u(t^k) - a_1(y_{N,M}^k(\mu), e^k(\mu), g_t^k(x;\mu) - g_{t,M}^k(x;\mu)) \\ & \quad \le \hat{\varepsilon}_{t,M}^k(\mu) \sup_{v\in X} \frac{f(v;q_{M+1})u(t^k) - a_1(y_{N,M}^k(\mu), v, q_{M+1})}{\|v\|_X}\|e^k(\mu)\|_X \\ & \quad \le \hat{\varepsilon}_{t,M}^k(\mu)\Phi_M^{\mathrm{na},k}(\mu)\|e^k(\mu)\|_X, \end{aligned} \quad (3.28)$$

and again from Young's inequality that

$$2\hat{\varepsilon}_{t,M}^k(\mu)\Phi_M^{\mathrm{na},k}(\mu)\|e^k(\mu)\|_X \le \frac{2}{\hat{\alpha}_a(\mu)}(\hat{\varepsilon}_{t,M}^k(\mu)\Phi_M^{\mathrm{na},k}(\mu))^2 + \frac{\hat{\alpha}_a(\mu)}{2}\|e^k(\mu)\|_X^2. \quad (3.29)$$

The desired results then directly follow from (3.26)–(3.29), invoking (3.5) and (3.20), and finally summing from $k' = 1$ to k with $e(\mu, t^0) = 0$. □

We note from (3.25) that our error bound comprises the affine as well as the nonaffine error contributions. We may thus choose N and M such that both contributions balance, i.e. neither N nor M should be chosen unnecessarily high. We also recall that our (crucial) assumption $g_t^k(x;\mu) \in W_{M+1}^{g_t}, 1 \le k \le K$, cannot be confirmed in actual practice — in fact, we generally have $g_t^k(x;\mu) \notin W_{M+1}^{g_t}$ and hence our error bound (3.25) is *not* completely rigorous, since $\hat{\varepsilon}_{t,M}^k(\mu) \le \varepsilon_{t,M}^k(\mu)$. We comment on both of these issues again in detail in Sec. 3.5 when discussing numerical results.

Finally, we note that the bound for the LTI case slightly simplifies due to the fact that the error estimator $\hat{\varepsilon}_M(\mu)$ is independent of time and can thus be pulled out of the summation.

We can now define the (simple) output bound in

Proposition 3.2. *Suppose that* $g_t^k(x;\mu) \in W_{M+1}^{g_t}$ *for* $1 \le k \le K$. *The error in the output of interest is then bounded by*

$$|s^k(\mu) - s_{N,M}^k(\mu)| \le \Delta_{N,M}^{s,k}(\mu), \quad \forall\, k \in \mathbb{K},\ \forall\, \mu \in \mathcal{D}, \tag{3.30}$$

where the output bound $\Delta_{N,M}^{s,k}(\mu)$ *is defined as*

$$\Delta_{N,M}^{s,k}(\mu) \equiv \sup_{v \in X} \frac{\ell(v)}{\|v\|_Y} \Delta_{N,M}^{y,k}(\mu). \tag{3.31}$$

Proof. From (1.2) and (3.11) we obtain

$$\begin{aligned} |s^k(\mu) - s_{N,M}^k(\mu)| &= |\ell(y^k(\mu)) - \ell(y_{N,M}^k(\mu))| \\ &= |\ell(e^k(\mu))| \le \sup_{v \in X} \frac{\ell(v)}{\|v\|_Y} \|e^k(\mu)\|_Y. \end{aligned}$$

The result immediately follows since $\|e^k(\mu)\|_Y \le \Delta_{N,M}^{y,k}(\mu)$, $1 \le k \le K$. □

3.3.3. *Computational procedure*

We now turn to the development of offline–online computational procedures for the calculation of $\Delta_{N,M}^{y,k}(\mu)$ and $\Delta_{N,M}^{s,k}(\mu)$. The necessary computations for the offline and online stage are detailed in Appendix A. Here, we only summarize the computational costs involved.

In the offline stage we first compute the quantities $\mathcal{F}$, $\mathcal{A}^{0,1}$, and $\mathcal{M}$ from (A.4) and (A.5) and then evaluate the necessary inner products. These operations require (to leading order) $O(M_{\max} N_{\max})$ expensive "truth" finite element solutions, and $O(M_{\max}^2 N_{\max}^2)$ $\mathcal{N}$-inner products. In the online stage — given a new parameter value μ and associated reduced basis solution $\underline{y}_{N,M}^k(\mu)$, $1 \le k \le K$ — the computational cost to evaluate $\Delta_{N,M}^{y,k}(\mu)$ and $\Delta_{N,M}^{s,k}(\mu)$, $1 \le k \le K$, is $O(KM^2N^2)$. Thus, all online calculations needed are *independent* of $\mathcal{N}$.

Concerning the LTI problem, we note that we can slightly lessen the computational cost by performing the M-dependent sums once before evaluating the dual norm at each timestep; the computational cost is thus $O(M^2N^2 + KN^2)$.

3.4. *Sampling procedure*

The sampling procedure is a two-stage process. We first construct the sample set $S_M^{g_t}$, associated space $W_M^{g_t}$, and set of interpolation points $T_M^{g_t}$ for the nonaffine function as described in Sec. 2. We then invoke a POD/Greedy sampling procedure — a combination of the Proper Orthogonal Decomposition (POD) in time with a Greedy selection procedure in parameter space[20,24] — to generate W_N^y. We first recall the function $\mathrm{POD}_X(\{y^k(\mu), 1 \le k \le K\}, R)$ which returns the R largest POD modes, $\{\chi_i, 1 \le i \le R\}$, now with respect to the X inner product.

The POD/Greedy procedure proceeds as follows: we first choose a $\mu^* \in \mathcal{D}$ and set $S_0^y = \{0\}$, $W_0^y = \{0\}$, $N = 0$. Then, for $1 \leq N \leq N_{\max}$, we first compute the projection error $e_{N,\text{proj}}^k(\mu) = y^k(\mu^*) - \text{proj}_{X,W_{N-1}^y}(y^k(\mu^*))$, $1 \leq k \leq K$, where $\text{proj}_{X,W_N}(w)$ denotes the X-orthogonal projection of $w \in X$ onto W_N, and we expand the parameter sample $S_N^y \leftarrow S_{N-1}^y \cup \{\mu^*\}$ and the reduced basis space $W_N^y \leftarrow W_{N-1}^y \cup \text{POD}_X(\{e_{N,\text{proj}}^k(\mu^*), 1 \leq k \leq K\}, 1)$, and set $N \leftarrow N+1$. Finally, we choose the next parameter value from $\mu^* \leftarrow \arg\max_{\mu \in \Xi_{\text{train}}} \Delta_{N,M_{\max}}^{y,K}(\mu) / |||\, y_N^K(\mu) |||$, i.e. we perform a greedy search over Ξ_{train} for the largest relative *a posteriori* error bound at the final time. Here, $\Xi_{\text{train}} \subset \mathcal{D}$ is a finite but suitably large train sample. In general, we may also specify a desired error tolerance, $\epsilon_{\text{tol,min}}$, and stop the procedure as soon as $\max_{\mu \in \Xi_{\text{train}}} \Delta_{N,M_{\max}}^{y,K}(\mu) / |||\, y_N^K(\mu) ||| \leq \epsilon_{\text{tol,min}}$ is satisfied; $N_{\max}$ is then indirectly determined through the stopping criterion.

During the POD/Greedy sampling procedure we shall use the "best" possible approximation $g_{t,M}^k(x;\mu)$ of $g_t^k(x;\mu)$ so as to minimize the error induced by the empirical interpolation procedure, i.e. we set $M = M_{\max}$.

For the model problem introduced in Sec. 3.1.2 the control input $u(t^k)$ was assumed to be known. In many instances, however, the control input may not be known *a priori* — a typical example is the application of reduced order models in a control setting. If the problem is linear time-invariant, we can appeal to the LTI property and generate the reduced basis space based on an impulse input in such cases.[19] Unfortunately, this approach will not work for LTV problems and nonlinear problems, i.e. a reduced basis space trained on an impulse response will, in general, not yield good approximation properties for arbitrary control inputs $u(t^k)$. One possible approach proposed in the literature is to train the reduced order model on a "generalized" impulse input, see Ref. 25. The idea here is to use a collection of "representative" control inputs, e.g. impulse and step functions of different magnitude shifted in time, in order to capture a richer dynamic behavior of the system. These ideas are, of course, heuristic and the treatment of unknown control inputs in the model reduction context is an open problem. However, our *a posteriori* error bound serves as a measure of fidelity especially in the online stage and we can thus detect an unacceptable deviation from the truth approximation in real-time.

3.5. *Numerical results*

We next present results for the model problem introduced in Sec. 3.1.2. We first consider the LTI problem and subsequently the LTV problem.

3.5.1. *The time-invariant case*

We construct the reduced basis space W_N^y according to the POD/Greedy sampling procedure in Sec. 3.4. To this end, we sample on Ξ_{train} with $M = M_{\max}$ and obtain $N_{\max} = 45$ for $\epsilon_{\text{tol,min}} = 1\text{E}{-6}$. We note from the definition of the X-inner product

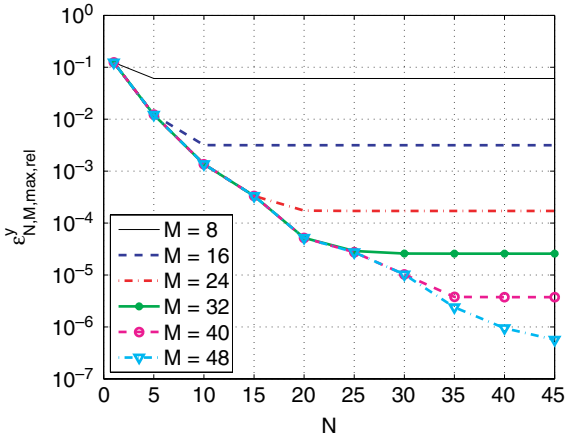

Fig. 3. LTI problem: convergence of the maximum relative error, $\epsilon^y_{N,M,\max,\mathrm{rel}}$.

and the fact that $G(x;\mu) > 0$, $\forall\, \mu \in \mathcal{D}$, that we can simply use $\hat{\alpha}_a(\mu) = 1$ as a lower bound for the coercivity constant.

In Fig. 3 we plot, as a function of N and M, the maximum relative error in the energy norm $\epsilon^y_{N,M,\max,\mathrm{rel}} = \max_{\mu\in\Xi_{\mathrm{Test}}} |||e^K(\mu)||| \,/\, |||\, y^K(\mu_y)|||$, where $\mu_y \equiv \arg\max_{\mu\in\Xi_{\mathrm{Test}}} |||y^K(\mu)|||$. We observe that the reduced basis approximation converges very rapidly. We also note the "plateau" in the curves for M fixed and the "drops" in the $N \to \infty$ asymptotes as M increases: for fixed M the error due to the coefficient function approximation, $g_M(x;\mu) - g(x;\mu)$, will ultimately dominate for large N; increasing M renders the coefficient function approximation more accurate, which in turn leads to a drop in the error. We further note that the separation points, or "knees", of the N-M-convergence curves reflect a balanced contribution of both error terms. At these points neither N nor M limit the convergence of the reduced basis approximation.

In Table 3 we present, as a function of N and M, $\epsilon^y_{N,M,\max,\mathrm{rel}}$, the maximum relative error bound $\Delta^y_{N,M,\max,\mathrm{rel}}$, and the average effectivity $\bar{\eta}^y_{N,M}$; here, $\Delta^y_{N,M,\max,\mathrm{rel}}$ is the maximum over Ξ_{Test} of $\Delta^{y,K}_{N,M}(\mu)/|||\, y^K(\mu_y)|||$ and $\bar{\eta}^y_{N,M}$ is the average over $\Xi_{\mathrm{Test}} \times \mathbb{I}$ of $\Delta^{y,k}_{N,M}(\mu)/|||y^k(\mu) - y^k_{N,M}(\mu)|||$. Note that the tabulated (N, M) values correspond roughly to the "knees" of the N-M-convergence curves. We observe very rapid convergence of the reduced basis approximation and error bound.

Table 3. LTI problem: convergence rates and effectivities as a function of N and M.

N	M	$\epsilon^y_{N,M,\max,\mathrm{rel}}$	$\Delta^y_{N,M,\max,\mathrm{rel}}$	$\bar{\eta}^y_{N,M}$	$\epsilon^s_{N,M,\max,\mathrm{rel}}$	$\Delta^s_{N,M,\max,\mathrm{rel}}$	$\bar{\eta}^s_{N,M}$
5	16	1.22E−02	1.74E−02	1.42	3.30E−03	1.01E−01	29.1
15	24	3.32E−04	4.75E−04	1.09	1.57E−04	2.77E−03	27.5
25	32	2.91E−05	4.30E−05	1.44	1.88E−05	2.50E−04	85.4
35	40	3.78E−06	3.50E−06	1.11	3.22E−06	2.04E−05	137
45	48	5.66E−07	8.17E−07	1.39	8.14E−08	4.76E−06	553

The effectivity serves as a measure of rigor and sharpness of the error bound: we would like $\bar{\eta}^y_{N,M} \geq 1$, i.e. $\Delta^{y,k}_{N,M}(\mu)$ be a true upper bound for the error in the energy-norm, and ideally we have $\bar{\eta}^y_{N,M} \approx 1$ so as to obtain a sharp bound for the error. We recall, however, that in actual practice we cannot confirm the assumption $g(x;\mu) \in W^g_{M+1}$ from Proposition 3.1 and thus $\bar{\eta}^y_{N,M} \geq 1$ may not hold. Specifically, if we choose (N, M) such that the function interpolation limits the convergence we do obtain effectivities less than 1, e.g. for $(N, M) = (25, 24)$ (instead of $(25, 32)$ in Table 3) we obtain $\bar{\eta}^y_{N,M} = 0.83$. A judicious choice for N and M is thus important for rigor and safety.

We next turn to the output estimate and present, in Table 3, the maximum relative output error $\epsilon^s_{N,M,\max,\text{rel}}$, the maximum relative output bound $\Delta^s_{N,M,\max,\text{rel}}$, and the average output effectivity $\bar{\eta}^s$. Here, $\epsilon^s_{N,M,\max,\text{rel}}$ is the maximum over Ξ_{Test} of $|s(\mu, t^k_s(\mu)) - s_{N,M}(\mu, t^k_s(\mu))|/|s(\mu, t^k_s(\mu))|$, $\Delta^s_{N,M,\max,\text{rel}}$ is the maximum over Ξ_{Test} of $\Delta^s_{N,M}(\mu, t^k_s(\mu))/|s(\mu, t^k_s(\mu))|$, and $\bar{\eta}^s$ is the average over Ξ_{Test} of $\Delta^s_{N,M}(\mu, t_\eta(\mu))/|s(\mu, t_\eta(\mu)) - s_{N,M}(\mu, t_\eta(\mu))|$, where $t^k_s(\mu) \equiv \arg\max_{t^k \in \mathbb{I}} |s(\mu, t^k)|$ and $t_\eta(\mu) \equiv \arg\max_{t^k \in \mathbb{I}} |s(\mu, t^k) - s_{N,M}(\mu, t^k)|$. Again, we observe very rapid convergence of the reduced basis output approximation and output bound — for only $N = 15$ and $M = 24$ the output error bound is already less than 0.3%. The output effectivities are still acceptable for smaller values of (N, M), but deteriorate for larger values.

In Table 4 we present, as a function of N and M, the online computational times to calculate $s^k_{N,M}(\mu)$ and $\Delta^{s,k}_{N,M}(\mu)$ for $1 \leq k \leq K$. The values are normalized with respect to the computational time for the direct calculation of the truth approximation output $s^k(\mu) = \ell(y^k(\mu)), 1 \leq k \leq K$. The computational savings for an accuracy of less than 0.3% ($N = 15$, $M = 24$) in the output bound is approximately a factor of 30. We note that the time to calculate $\Delta^{s,k}_{N,M}(\mu)$ exceeds that of calculating $s^k_N(\mu)$ — this is due to the higher computational cost, $O(M^2N^2 + KN^2)$, to evaluate $\Delta^{y,k}_{N,M}(\mu)$. Thus, although our previous observation suggests to choose M large so that the error contribution due to the nonaffine function approximation is small, we should choose M as small as possible to retain the computational efficiency of our method. We emphasize that the reduced basis entry does *not* include the extensive offline computations — and is thus only meaningful in the real-time or many-query contexts.

Table 4. LTI problem: online computational times (normalized with respect to the time to solve for $s^k(\mu), 1 \leq k \leq K$).

N	M	$s^k_{N,M}(\mu), \forall\, k \in \mathbb{K}$	$\Delta^{s,k}_{N,M}(\mu), \forall\, k \in \mathbb{K}$	$s^k(\mu), \forall\, k \in \mathbb{K}$
5	16	2.70E−03	1.84E−02	1
15	24	3.18E−03	3.01E−02	1
25	32	3.96E−03	4.57E−02	1
35	40	4.71E−03	7.16E−02	1
45	48	5.52E−03	1.02E−01	1

3.5.2. *The time-varying case*

We next consider the LTV problem and first recall the results for the nonaffine time-varying function approximation in Sec. 2.2.3. We perform the POD/Greedy sampling procedure from Sec. 3.4 to generate the reduced basis space. To this end, we sample on Ξ_{train} with $M = M_{\max}$ and obtain $N_{\max} = 39$ for $\epsilon_{\text{tol,min}} = 1\text{E}{-}6$. We may again use $\hat{\alpha}_a(\mu) = 1$ as a lower bound for the coercivity constant. Note that the quantities presented here are defined analogous to the quantities presented for the LTI problem.

In Fig. 4 we plot, as a function of N and M, the maximum relative error in the energy norm $\epsilon^y_{N,M,\text{max,rel}}$. We observe that the reduced basis approximation converges very rapidly and the curves show the same behavior as in the LTI case. A balanced contribution of both error terms is important to not limit the convergence of the approximation and thus to guarantee computational efficiency.

In Table 5 we present, as a function of N and M, $\epsilon^y_{N,M,\text{max,rel}}$, the maximum relative error bound $\Delta^y_{N,M,\text{max,rel}}$, the average effectivity $\bar{\eta}^y_{N,M}$, the maximum relative output error $\epsilon^s_{N,M,\text{max,rel}}$, the maximum relative output bound $\Delta^s_{N,M,\text{max,rel}}$, and the average output effectivity $\bar{\eta}^s$. Again, the tabulated (N, M) values correspond

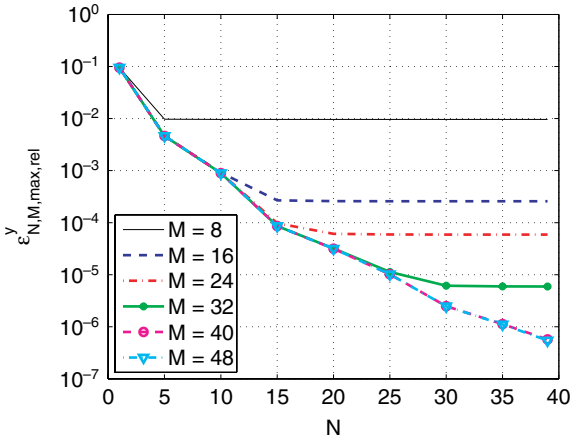

Fig. 4. LTV problem: convergence of the maximum relative error $\epsilon^y_{N,M,\text{max,rel}}$.

Table 5. LTV problem: convergence rates and effectivities as a function of N and M.

N	M	$\epsilon^y_{N,M,\text{max,rel}}$	$\Delta^y_{N,M,\text{max,rel}}$	$\bar{\eta}^y_{N,M}$	$\epsilon^s_{N,M,\text{max,rel}}$	$\Delta^s_{N,M,\text{max,rel}}$	$\bar{\eta}^s_{N,M}$
5	8	9.72E−03	6.27E−02	0.64	1.17E−02	2.46E−02	1.64
10	16	9.13E−04	1.29E−03	1.44	2.68E−04	5.05E−03	34.8
15	24	9.75E−05	1.28E−04	1.32	6.48E−05	5.03E−04	16.7
25	32	1.13E−05	1.54E−05	1.19	6.99E−06	6.03E−05	7.28
35	40	1.13E−06	1.64E−06	1.44	1.38E−07	6.44E−06	64.0

Table 6. LTV problem: online computational times (normalized with respect to the time to solve for $s^k(\mu), 1 \le k \le K$).

N	M	$s^k_{N,M}(\mu), \forall\, k \in \mathbb{K}$	$\Delta^{s,k}_{N,M}(\mu), \forall\, k \in \mathbb{K}$	$s^k(\mu), \forall\, k \in \mathbb{K}$
5	8	1.35E−04	2.18E−03	1
10	16	1.92E−04	8.18E−03	1
15	24	2.86E−04	1.99E−02	1
25	32	4.48E−04	3.85E−02	1
35	40	7.07E−04	6.52E−02	1

roughly to the "knees" of the N-M-convergence curves. We observe very rapid convergence of the reduced basis (output) approximation and (output) error bound. We obtain an average effectivity of less than one for $(N, M) = (5, 8)$, showing that our assumption in Corollary 2.1 is not satisfied in general. However, for all other values of N and M tabulated our *a posteriori* error bounds do provide an upper bound for the true error. Furthermore, our bounds for the error in the energy norm and the output are very sharp for all values of (N, M).

Finally, we present the online computational times to calculate $s^k_{N,M}(\mu)$ and $\Delta^{s,k}_{N,M}(\mu)$ for $1 \le k \le K$ in Table 6. The values are normalized with respect to the computational time for the direct calculation of the truth approximation output $s^k(\mu) = \ell(y^k(\mu)), 1 \le k \le K$. The computational savings for an accuracy of approximately 0.5% ($N = 10$, $M = 16$) in the output bound is approximately a factor of 120. As we already observed in the LTI case, the time to calculate $\Delta^{s,k}_{N,M}(\mu)$ exceeds that of calculating $s^k_N(\mu)$ due to the higher computational cost for the bound calculation. Even though the computational cost to evaluate the error bound in the LTV case is higher than in the LTI case (see Sec. 3.3.3), the savings with respect to the truth approximation are still larger here. The reason is that solving the truth approximation requires a matrix assembly of the nonaffine terms at every timestep.

4. Nonlinear Parabolic Equations

In this section we extend the previous results to nonaffine *nonlinear* parabolic problems. We first introduce the abstract statement and reduced basis approximation, we then develop the *a posteriori* error bounds and subsequently introduce a new procedure — based on the POD/Greedy-EIM algorithm of Sec. 2.2.1 — to define the generating functions for the nonlinear term. Finally, we discuss numerical results obtained for a model problem.

4.1. *Problem statement*

4.1.1. *Abstract formulation*

We consider a time-discrete framework associated to the time interval $I \equiv]0, t_f]$ as introduced in Sec. 1: $\bar{I}$ is divided into K subintervals of equal length $\Delta t = \frac{t_f}{K}$ and

t^k is defined by $t^k \equiv k\Delta t$, $0 \le k \le K \equiv \frac{t_f}{\Delta t}$; furthermore, $\mathbb{I} \equiv \{t^0, \ldots, t^k\}$ and $\mathbb{K} \equiv \{1, \ldots, K\}$. The "truth" approximation is then: given a parameter $\mu \in \mathcal{D}$, we evaluate the output of interest

$$s^k(\mu) = \ell(y^k(\mu)), \quad \forall\, k \in \mathbb{K}, \tag{4.1}$$

where the field variable $y^k(\mu) \in X$, $1 \le k \le K$, satisfies the weak form of the nonlinear parabolic partial differential equation

$$\begin{aligned} m(y^k(\mu), v) + \Delta t a^L(y^k(\mu), v) + \Delta t \int_\Omega g(y^k(\mu); x; \mu) v \\ = m(y^{k-1}(\mu), v) + \Delta t f(v) u(t^k), \quad \forall\, v \in X, \end{aligned} \tag{4.2}$$

with initial condition (say) $y(\mu, t^0) = 0$. Here, μ and $\mathcal{D}$ are the input and input domain and $u(t^k)$ denotes the control input. The function $g(w; x; \mu) : \mathbb{R} \times \Omega \times \mathcal{D} \to \mathbb{R}$ is a nonlinear nonaffine function continuous in its arguments, increasing in its first argument, and satisfies, for all $y \in \mathbb{R}, yg(y; x; \mu) \ge 0$ for any $x \in \Omega$ and $\mu \in \mathcal{D}$. We note that the field variable, $y^k(\mu)$, is of course also a function of the spatial coordinate x. In the sequel we will use the notation $y(x, t^k; \mu)$ to signify this dependence whenever it is crucial.

We shall make the following assumptions. We assume that $a^L(\cdot, \cdot)$ and $m(\cdot, \cdot)$ are continuous

$$a^L(w, v) \le \gamma_a^0 \|w\|_X \|v\|_X, \quad \forall\, w, v \in X, \tag{4.3}$$

$$m(w, v) \le \gamma_m^0 \|w\|_Y \|v\|_Y, \quad \forall\, w, v \in X; \tag{4.4}$$

coercive,

$$0 < \alpha_a^0 \equiv \inf_{w \in X} \frac{a^L(w, w)}{\|w\|_X^2}, \tag{4.5}$$

$$0 < \alpha_m^0 \equiv \inf_{v \in X} \frac{m(v, v)}{\|v\|_Y^2}; \tag{4.6}$$

and symmetric, $a^L(v, w) = a^L(w, v), \forall\, w, v \in X$, and $m(v, w) = m(w, v), \forall\, w, v \in X$. (We (plausibly) suppose that $\gamma_a^0, \gamma_m^0, \alpha_a^0, \alpha_m^0$ may be chosen independent of $\mathcal{N}$.) We also require that the linear forms $f(\cdot) : X \to \mathbb{R}$ and $\ell(\cdot) : X \to \mathbb{R}$ be bounded with respect to $\|\cdot\|_Y$. The problem is thus well-posed.[26]

Since the focus of this section is the treatment of the nonlinearity $g(w; x; \mu)$ we assume that the bilinear and linear forms m, a^L and b, ℓ are parameter-independent; a parameter dependence of either form is readily admitted. Note also that our results presented here directly carry over to the case where g is also an explicit function of (discrete) time t^k.

4.1.2. *Model problem*

We turn to a numerical example first introduced in Ref. 18. We consider the following nonlinear diffusion problem defined on the unit square, $\Omega =]0, 1[^2 \in \mathbb{R}^2$: Given

$\mu = (\mu_1, \mu_2) \in \mathcal{D} \equiv [0.01, 10]^2$, we evaluate $y^k(\mu) \in X$ from (4.2), where $X \subset X^e \equiv H_0^1(\Omega)$ is a linear finite element truth approximation subspace of dimension $\mathcal{N} = 2601$,

$$m(w,v) \equiv \int_\Omega wv, \quad a^L(w,v) \equiv \int_\Omega \nabla w \cdot \nabla v,$$
$$f(v) \equiv 100 \int_\Omega v \sin(2\pi x_1)\cos(2\pi x_2), \tag{4.7}$$

and the nonlinearity is given by

$$g(y^k(\mu);\mu) = \mu_1 \frac{e^{\mu_2 y^k(\mu)} - 1}{\mu_2}. \tag{4.8}$$

The output $s^k(\mu)$ is evaluated from (4.1) with $\ell(v) = \int_\Omega v$. We presume the periodic control input $u(t^k) = \sin(2\pi t^k), t^k \in \mathbb{I}$. We shall consider the time interval $\bar{I} = [0, 2]$ and a timestep $\Delta t = 0.01$; we thus have $K = 200$.

We note that μ_2 represent the strength of the nonlinearity whereas μ_1 represents the strength of the sink term in (4.8); as $\mu_2 \to 0$ we have $g(w;\mu) \to \mu_1 w$. The solution thus tends to the solution for the linear problem as μ_2 tends to zero. Two snapshots of the solution $y^k(\mu)$ at time $t^k = 25\Delta t$ are shown for $\mu = (0.01, 0.01)$ and $\mu = (10, 10)$ in Figs. 5(a) and 5(b), respectively. We observe that the solution has two negative peaks and two positive peaks with similar height for $\mu = (0.01, 0.01)$ (which oscillate back and forth in time). As μ_2 increases, the height of the negative peaks remains largely unchanged, while the positive peaks get rectified as shown in Fig. 5(b). The exponential nonlinearity has a damping effect on the positive part of $y^k(\mu)$, but has (almost) no effect on the negative part. Note that the solution for $\mu = (10, 10)$, of course, also oscillates in time — with the positive peaks always being smaller than the negative peaks.

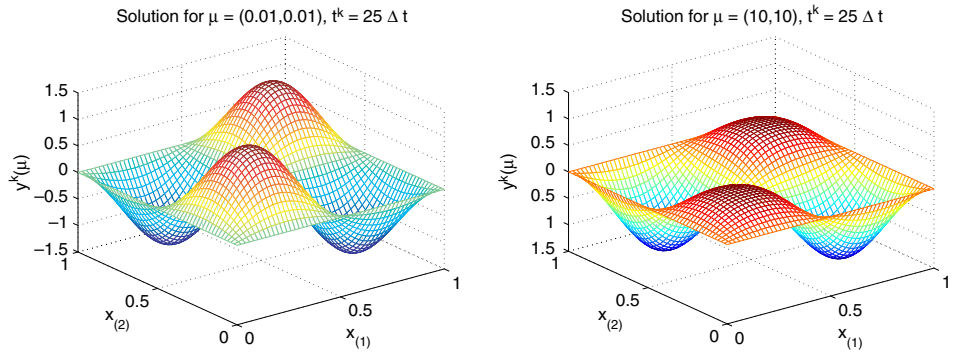

(a) (b)

Fig. 5. Solution $y^k(\mu)$ at $t^k = 25\Delta t$ for (a) $\mu = (-1, -1)$ and (b) $\mu = (-0.01, -0.01)$.

4.2. *Reduced basis approximation*

4.2.1. *Formulation*

We assume that we are given the nested collateral reduced basis space $W_M^g = \text{span}\{\xi_n, 1 \le n \le M\} = \text{span}\{q_1, \ldots, q_M\}, 1 \le M \le M_{\max}$, and nested set of interpolation points $T_M^g = \{x_1, \ldots, x_M\}, 1 \le M \le M_{\max}$. We will propose a procedure to construct W_M^g and T_M^g in Sec. 4.4. Then, for given $w^k(\mu) \in X$ and M, we approximate $g(w^k(\mu); x; \mu)$ by $g_M^{w^k}(x; \mu) = \sum_{m=1}^M \varphi_{Mm}^k(\mu) q_m(x)$, where

$$\sum_{j=1}^M B_{ij}^M \varphi_{Mj}^k(\mu) = g(w(x_i, t^k; \mu); x_i; \mu), \quad 1 \le i \le M; \tag{4.9}$$

note that $\varphi_M^k(\mu) \equiv \varphi_M(t^k; \mu)$ also depends on the (discrete) time t^k. We also introduce the nested Lagrangian reduced basis spaces $W_N^y = \text{span}\{\zeta_n, 1 \le n \le N\}, 1 \le N \le N_{\max}$, where the $\zeta_n, 1 \le n \le N$, are mutually $(\cdot, \cdot)_X$-orthogonal basis functions. We construct W_N^y according to the POD/Greedy procedure outlined in Sec. 3.4 with $M = M_{\max}$.

Our reduced basis approximation $y_{N,M}^k(\mu)$ to $y^k(\mu)$ is then obtained by a standard Galerkin projection: given $\mu \in \mathcal{D}$, $y_{N,M}^k(\mu) \in W_N^y$ satisfies

$$\begin{aligned} &m(y_{N,M}^k(\mu), v) + \Delta t a^L(y_{N,M}^k(\mu), v) + \Delta t \int_\Omega g_M^{y_{N,M}^k}(x; \mu) v \\ &\quad = m(y_{N,M}^{k-1}(\mu), v) + \Delta t f(v) u(t^k), \quad \forall\, v \in W_N^y, \ \forall\, k \in \mathbb{K}, \end{aligned} \tag{4.10}$$

with initial condition $y_{N,M}(\mu, t^0) = 0$. We evaluate the output approximation from

$$s_{N,M}^k(\mu) = \ell(y_{N,M}^k(\mu)), \quad \forall\, k \in \mathbb{K}. \tag{4.11}$$

We note that the need to incorporate the empirical interpolation method into the reduced basis approximation only exists for high-order polynomial or non-polynomial nonlinearities.[18] If g is a low-order (or at most quadratically) polynomial nonlinearity in $y^k(\mu)$, we can expand the nonlinear terms into their power series and develop an efficient, i.e. online $\mathcal{N}$-independent, offline–online computational decomposition using the standard Galerkin procedure.[46,47]

4.2.2. *Computational procedure*

In this section we develop the offline–online computational decomposition to recover online $\mathcal{N}$-independence even in the nonlinear case. We first express $y_{N,M}^k(\mu)$ as

$$y_{N,M}^k(\mu) = \sum_{n=1}^N y_{N,Mn}^k(\mu) \zeta_n, \tag{4.12}$$

and choose as test functions $v = \zeta_j, 1 \le j \le N$, in (4.10).

It then follows from the affine representation of $g_M^{y_{N,M}^k}$ that $\underline{y}_{N,M}^k(\mu) = [y_{N,M1}^k(\mu)\, y_{N,M2}^k(\mu) \cdots y_{N,MN}^k(\mu)]^T \in \mathbb{R}^N$, $1 \le k \le K$, satisfies

$$(M_N + \Delta t A_N)\underline{y}_{N,M}^k(\mu) + \Delta t C^{N,M}\varphi_M^k(\mu) = M_N \underline{y}_{N,M}^{k-1}(\mu) + \Delta t B_N u(t^k), \qquad (4.13)$$

with initial condition $y_{N,Mn}(t^0;\mu) = 0, 1 \le n \le N$. Here, the coefficients $\varphi_M^k(\mu) = [\varphi_{M1}^k(\mu)\ \varphi_{M2}^k(\mu) \cdots \varphi_{MM}^k(\mu)]^T \in \mathbb{R}^M$ are determined from (4.9) with $w^k = y_{N,M}^k$; $M_N \in \mathbb{R}^{N\times N}$, $A_N \in \mathbb{R}^{N\times N}$, and $C^{N,M} \in \mathbb{R}^{N\times M}$, are *parameter-independent* matrices with entries $M_{Ni,j} = m(\zeta_j, \zeta_i), 1 \le i, j \le N$, $A_{Nj,i} = a(\zeta_j, \zeta_i), 1 \le i, j \le N$, and $C_{i,j}^{N,M} = \int_\Omega q_j \zeta_i, 1 \le i \le N, 1 \le j \le M$, respectively; and $F_N \in \mathbb{R}^N$ is a *parameter-independent* vector with entries $F_{Ni} = f(\zeta_i), 1 \le i \le N$.

We can now substitute $\varphi_{Mm}^k(\mu)$ from (4.9) into (4.13) to obtain the nonlinear algebraic system

$$\begin{aligned}(M_N + \Delta t A_N)\underline{y}_{N,M}^k(\mu) &+ \Delta t D^{N,M} g(Z^{N,M}\underline{y}_{N,M}^k(\mu); \underline{x}_M; \mu) \\ &= M_N \underline{y}_{N,M}^{k-1}(\mu) + \Delta t B_N u(t^k), \quad \forall\, k \in \mathbb{K}, \end{aligned} \qquad (4.14)$$

where $D^{N,M} = C^{N,M}(B^M)^{-1} \in \mathbb{R}^{N\times M}$, $Z^{N,M} \in \mathbb{R}^{M\times N}$ is a *parameter-independent* matrix with entries $Z_{i,j}^{N,M} = \zeta_j(x_i), 1 \le i \le M, 1 \le j \le N$, and $\underline{x}_M = [x_i \ldots x_M]^T \in \mathbb{R}^M$ is the set of interpolation points. We now solve for $\underline{y}_{N,M}^k(\mu)$ at each timestep using a Newton iterative scheme[b]: given the solution for the previous timestep, $\underline{y}_{N,M}^{k-1}(\mu)$, and a current iterate $\underline{\bar{y}}_{N,M}^k(\mu)$, we find an increment $\delta \underline{y}_{N,M}$ such that

$$\begin{aligned}(M_N + \Delta t A_N + \Delta t \bar{E}^N)&\delta \underline{y}_{N,M} \\ &= M_N \underline{y}_{N,M}^{k-1}(\mu) + \Delta t B_N(\mu) u(t^k) - (M_N + \Delta t A_N)\underline{\bar{y}}_{N,M}^k(\mu) \\ &\quad - \Delta t D^{N,M} g(Z^{N,M}\underline{\bar{y}}_{N,M}^k(\mu); \underline{x}_M; \mu), \end{aligned} \qquad (4.15)$$

where $\bar{E}^N \in \mathbb{R}^{N\times N}$ must be calculated at every Newtoniteration from

$$\bar{E}_{i,j}^N = \sum_{m=1}^M D_{i,m}^{N,M} g_1\left(\sum_{n=1}^N \bar{y}_{N,Mn}^k(\mu)\zeta_n(x_m); x_m; \mu\right)\zeta_j(x_m), \quad 1 \le i,\ j \le N, \qquad (4.16)$$

where g_1 is the partial derivative of g with respect to the first argument. Finally, we evaluate the output estimate from

$$s_{N,M}^k(\mu) = L_N^T \underline{y}_{N,M}^k(\mu), \quad \forall\, k \in \mathbb{K}, \qquad (4.17)$$

where $L_N \in \mathbb{R}^N$ is the output vector with entries $L_{Ni} = \ell(\zeta_i), 1 \le i \le N$.

[b]We note that (4.14) is not necessarily well-posed and that we currently do not have an *a priori* criterion to check for well-posedness before the Newton iteration.

The offline–online decomposition is now clear. In the offline stage — performed only *once* — we first construct the nested approximation spaces W_M^g and sets of interpolation points $T_M^g, 1 \le M \le M_{\max}$. We then solve for the $\zeta_n, 1 \le n \le N_{\max}$ and compute and store the μ-independent quantities M_N, A_N, B^M, $D^{N,M}$, B_N and $Z^{N,M}$. In the online stage — performed many times, for each new parameter value μ — we solve (4.15) for $\underline{y}_{N,M}^k(\mu)$ and evaluate the output estimate $s_{N,M}^k(\mu)$ from (4.17). The operation count is dominated by the Newton update at each timestep: we first assemble $\bar{E}^N$ from (4.16) at cost $O(MN^2)$ — note that we perform the sum in the parenthesis of (4.16) first before performing the outer sum — and then invert the left-hand side of (4.15) at cost $O(N^3)$. The operation count in the online stage is thus $O(MN^2 + N^3)$ per Newton iteration per timestep. We thus recover $\mathcal{N}$-independence in the online stage.

4.3. A posteriori *error estimation*

4.3.1. *Preliminaries*

We now turn to the development of our *a posteriori* error estimator; by construction, the error estimator is rather similar to the nonaffine parabolic case in Sec. 3. To begin, we recall that the bilinear form a^L is assumed to be parameter-independent here. We can thus use the coercivity constant α_a and have no need for the lower bound $\hat{\alpha}_a(\mu)$ required earlier. We next introduce the dual norm of the residual

$$\varepsilon_{N,M}^k(\mu) \equiv \sup_{v \in X} \frac{R^k(v;\mu)}{\|v\|_X}, \quad \forall\, k \in \mathbb{K}, \tag{4.18}$$

where

$$R^k(v;\mu) \equiv f(v)u(t^k) - \frac{1}{\Delta t} m(y_{N,M}^k(\mu) - y_{N,M}^{k-1}(\mu), v) - a^L(y_{N,M}^k(\mu), v) - \int_\Omega g_M^{y_{N,M}^k}(x;\mu) v, \quad \forall\, v \in X,\ \forall\, k \in \mathbb{K}, \tag{4.19}$$

is the residual associated to the nonlinear parabolic problem. We also require the dual norm

$$\vartheta_M^q \equiv \sup_{v \in X} \frac{\int_\Omega q_{M+1} v}{\|v\|_X} \tag{4.20}$$

and the error bound $\hat{\varepsilon}_M^k(\mu)$ for the nonlinear function approximation given by

$$\hat{\varepsilon}_M^k(\mu) \equiv |g(y_{N,M}^k(x_{M+1};\mu); x_{M+1};\mu) - g_M^{y_{N,M}^k}(x_{M+1};\mu)|. \tag{4.21}$$

Finally, we define the "spatio-temporal" energy norm $|||v^k(\mu)|||^2 \equiv m(v^k(\mu), v^k(\mu)) + \sum_{k'=1}^k a^L(v^{k'}(\mu), v^{k'}(\mu))\Delta t, \forall\, v \in X, \forall\, k \in \mathbb{K}$.

4.3.2. *Error bound formulation*

We obtain the following result for the error in the energy norm.

Proposition 4.1. *Suppose that* $g(y^k_{N,M}(\mu); x; \mu) \in W^g_{M+1}, 1 \le k \le K$. *The error,* $e^k(\mu) \equiv y^k(\mu) - y^k_{N,M}(\mu)$, *is then bounded by*

$$|||e^k(\mu)||| \le \Delta^{y,k}_{N,M}(\mu), \quad \forall\, \mu \in \mathcal{D},\ \forall\, k \in \mathbb{K}, \tag{4.22}$$

where the error bound $\Delta^{y,k}_{N,M}(\mu)$ *is defined as*

$$\Delta^{y,k}_{N,M}(\mu) \equiv \left(\frac{2\Delta t}{\alpha_a} \sum_{k'=1}^{k} \varepsilon^{k'}_{N,M}(\mu)^2 + \frac{2\Delta t}{\alpha_a} \vartheta^q_M{}^2 \sum_{k'=1}^{k} \hat{\varepsilon}^{k'}_M(\mu)^2 \right)^{\frac{1}{2}}. \tag{4.23}$$

Proof. We immediately derive from (4.2) and (4.19) that $e^k(\mu) = y^k(\mu) - y^k_{N,M}(\mu)$, $1 \le k \le K$, satisfies

$$\begin{aligned} &m(e^k(\mu), v) + \Delta t a^L(e^k(\mu), v) + \Delta t \int_\Omega (g(y^k(\mu); x; \mu) - g(y^k_{N,M}(\mu); x; \mu))v \\ &\quad = m(e^{k-1}(\mu), v) + \Delta t R(v; \mu, t^k) \\ &\qquad + \Delta t \int_\Omega \left(g_M^{y^k_{N,M}}(x; \mu) - g(y^k_{N,M}(\mu); x; \mu) \right) v, \quad \forall\, v \in X, \end{aligned} \tag{4.24}$$

where $e(t^0; \mu) = 0$ since $y(t^0; \mu) = y_{N,M}(t^0; \mu) = 0$ by assumption. We now choose $v = e^k(\mu)$ in (4.24), immediately note from the monotonicity of g that

$$\int_\Omega (g(y^k(\mu); x; \mu) - g(y^k_{N,M}(\mu); x; \mu))e^k(\mu) \ge 0; \tag{4.25}$$

invoke (4.18) and the Cauchy–Schwarz inequality for the cross term $m(e^{k-1}(\mu), e^k(\mu))$ to obtain, for $1 \le k \le K$,

$$\begin{aligned} &m(e^k(\mu), e^k(\mu)) + \Delta t a^L(e^k(\mu), e^k(\mu)) \\ &\quad \le m^{\frac{1}{2}}(e^{k-1}(\mu), e^{k-1}(\mu)) m^{\frac{1}{2}}(e^k(\mu), e^k(\mu)) + \Delta t \varepsilon^k_{N,M}(\mu) \|e^k(\mu)\|_X \\ &\qquad + \Delta t \int_\Omega \left(g_M^{y^k_{N,M}}(x; \mu) - g(y^k_{N,M}(\mu); x; \mu) \right) e^k(\mu). \end{aligned} \tag{4.26}$$

We now recall Young's inequality (for $c \in \mathbb{R}, d \in \mathbb{R}, \rho \in \mathbb{R}_+$)

$$2|c||d| \le \frac{1}{\rho^2} c^2 + \rho^2 d^2, \tag{4.27}$$

which we apply twice: first, choosing $c = m^{\frac{1}{2}}(e^k(\mu), e^k(\mu))$, $d = m^{\frac{1}{2}}(e^{k-1}(\mu), e^{k-1}(\mu))$, and $\rho = 1$, we obtain

$$\begin{aligned} &2m^{\frac{1}{2}}(e^k(\mu), e^k(\mu)) m^{\frac{1}{2}}(e^{k-1}(\mu), e^{k-1}(\mu)) \\ &\quad \le m(e^{k-1}(\mu), e^{k-1}(\mu)) + m(e^k(\mu), e^k(\mu)); \end{aligned} \tag{4.28}$$

and second, choosing $c = \varepsilon^k_{N,M}(\mu)$, $d = \|e^k(\mu)\|_X$, and $\rho = (\alpha_a/2)^{\frac{1}{2}}$ we have

$$2\varepsilon^k_{N,M}(\mu)\|e^k(\mu)\|_X \leq \frac{2}{\alpha_a}\varepsilon^k_{N,M}(\mu)^2 + \frac{\alpha_a}{2}\|e^k(\mu)\|^2_X. \tag{4.29}$$

We now note from our assumption $g(y^k_{N,M}(\mu); x; \mu) \in W^g_{M+1}$ and Proposition 2.1 that

$$g_M^{y^k_{N,M}}(x;\mu) - g(y^k_{N,M}(\mu); x; \mu) = \hat{\varepsilon}^k_M(\mu) q_{M+1}(x); \tag{4.30}$$

it thus follows that

$$\begin{aligned}
&2\int_\Omega \left(g_M^{y^k_{N,M}}(x;\mu) - g(y^k_{N,M}(\mu); x; \mu) \right) e^k(\mu) \\
&\quad \leq 2 \sup_{v\in X} \left\{ \frac{\int_\Omega \left(g_M^{y^k_{N,M}}(x;\mu) - g(y^k_{N,M}(\mu); x; \mu) \right) v}{\|v\|_X} \right\} \|e^k(\mu)\|_X \\
&\quad \leq 2\hat{\varepsilon}^k_M(\mu) \sup_{v\in X} \left\{ \frac{\int_\Omega q_{M+1} v}{\|v\|_X} \right\} \|e^k(\mu)\|_X \\
&\quad \leq 2\hat{\varepsilon}^k_M(\mu)\vartheta^q_M \ \|e^k(\mu)\|_X \\
&\quad \leq \frac{2}{\alpha_a}\hat{\varepsilon}^k_M(\mu)^2 {\vartheta^q_M}^2 + \frac{\alpha_a}{2}\|e^k(\mu)\|^2_X,
\end{aligned} \tag{4.31}$$

where we applied (4.27) with $c = \hat{\varepsilon}^k_M(\mu)\vartheta^q_M$, $d = \|e^k(\mu)\|_X$, and $\rho = (\alpha_a/2)^{\frac{1}{2}}$ in the last step. Finally, from (4.26), (4.28), (4.29), (4.31), invoking (4.5) and summing from 1 to k we obtain the bound

$$\begin{aligned}
&m(e^k(\mu), e^k(\mu)) + \Delta t \sum_{k'=1}^k a(e^{k'}(\mu), e^{k'}(\mu)) \\
&\qquad \leq \frac{2\Delta t}{\alpha_a} \sum_{k'=1}^k \left(\varepsilon^{k'}_{N,M}(\mu) 2 + {\vartheta^q_M}^2 \hat{\varepsilon}^{k'}_M(\mu)^2 \right)
\end{aligned} \tag{4.32}$$

which is the result stated in Proposition 4.1. □

We can now define the (simple) output bound

Proposition 4.2. *Suppose that $g(y^k_{N,M}(\mu); x; \mu) \in W^g_{M+1}, 1 \leq k \leq K$. The error in the output is then bounded by*

$$|s^k(\mu) - s^k_{N,M}(\mu)| \leq \Delta^{s,k}_{N,M}(\mu), \quad \forall\, k \in \mathbb{K}, \ \forall\, \mu \in \mathcal{D}, \tag{4.33}$$

where the output bound is defined as

$$\Delta^{s,k}_{N,M}(\mu) \equiv \sup_{v\in X} \frac{\ell(v)}{\|v\|_Y} \Delta^{y,k}_{N,M}(\mu), \quad \forall\, k \in \mathbb{K}, \ \forall\, \mu \in \mathcal{D}. \tag{4.34}$$

Proof. The result directly follows from (4.1), (4.11), and the fact that the error satisfies $\|e^k(\mu))\|_Y \leq \Delta^{y,k}_{N,M}(\mu)$, $1 \leq k \leq K$, for all $\mu \in \mathcal{D}$. □

We note from (4.23) that our error bound comprises two terms: the contribution from the linear (affine) terms and from the nonlinear (nonaffine) function approximation. Similar to the linear nonaffine case, we may thus choose N and M such that both contributions balance, i.e. neither N nor M should be chosen unnecessarily high. However, our choice should also take the rigor of the error bound into account.

The rigor is related to the condition that $g(y^k_{N,M}(\mu); x; \mu) \in W^g_{M+1}, 1 \le k \le K$, which is very unlikely to hold in the nonlinear case: first, because W^g_M is constructed based on $g(y^k(\mu); x; \mu)$ and not $g(y^k_{N,M}(\mu); x; \mu)$, and second, particularly because of the time-dependence of $g(y^k_{N,M}(\mu); x; \mu)$. A judicious choice of N and M can control the trade-off between safety and efficiency — we opt for safety by choosing N and M such that the rigorous part $\varepsilon^k_{N,M}(\mu)$ dominates over the non-rigorous part, $\vartheta^q_M \hat{\varepsilon}^k_M(\mu)$; we opt for efficiency by choosing N and M such that both terms balance.

4.3.3. *Computational procedure*

The offline–online decomposition for the calculation of $\Delta^{y,k}_{N,M}(\mu)$ (and $\Delta^{s,k}_{N,M}(\mu)$) follows directly from the corresponding procedure for nonaffine problems discussed in Sec. 3.3.3. We will therefore omit the details and only summarize the computational costs involved in the online stage. In the online stage — given a new parameter value μ and associated reduced basis solution $\underline{y}^k_{N,M}(\mu), 1 \le k \le K$ — the computational cost to evaluate $\Delta^{y,k}_{N,M}(\mu)$ (and hence $\Delta^{s,k}_{N,M}(\mu)$) is $O(K(N+M)^2)$ and thus *independent* of $\mathcal{N}$.

4.4. *Sampling procedure*

We first consider the construction of W^g_M and T^g_M. We recall that our previous approach of constructing the collateral reduced basis space W^g_M in the nonlinear case is computationally very expensive.[18] The reason is twofold: first, we need to calculate and store the "truth" solution $y^k(\mu)$ at all times $t^k \in \mathbb{I}$ on the training sample Ξ^g_{train} in parameter space. And second, construction of W^g_M requires the solution of a linear program[c] for all parameter-time pairs, $(t^k; \mu) \in \tilde{\Xi}^g_{\text{train}} \equiv \mathbb{I} \times \Xi^g_{\text{train}}$, since the function g is time-varying, as is inherently the case in the nonlinear context.

Our new approach is straightforward: we simply apply the POD/Greedy-EIM procedure introduced in Sec. 2.2.1 to the nonlinear (time-varying) function $g(y^k(\mu); x; \mu)$. Although we cannot avoid the first problem related to our previous construction, i.e. calculation and storage of $y^k(\mu)$ on Ξ^g_{train}, we do to a great extent

[c]The construction of W^g_M in Ref. 18 is based on a Greedy selection process: we choose the next parameter value μ^* — and hence generating function $\xi \equiv g(y^k(\mu^*); x; \mu)$ — as the one that maximizes the best approximation error in the $L^\infty(\Omega)$-norm over the train sample.

alleviate the second problem. Furthermore, we believe that our new approach is more coherent — as compared to the construction of W_N^y — and more robust.

Given W_M^g, T_M^g, and B^M, we can then construct W_N^y following the POD/Greedy procedure outlined in Sec. 3.4. We shall again use the "best" possible approximation $g_M^{y_{N,M}^k}(x;\mu)$ of $g(y_{N,M}^k;x;\mu)$ so as to minimize the error induced by the empirical interpolation procedure, i.e. we set $M = M_{\max}$.

4.5. *Numerical results*

We now present numerical results for the model problem introduced in Sec. 4.1.2. We choose for $\Xi_{\text{train}} \subset \mathcal{D}$ a deterministic grid of 12×12 parameter points over $\mathcal{D}$ and we take $\mu_1^g = (10, 10)$. Next, we pursue the POD/Greedy-EIM procedure described in Sec. 4.4 to construct S_M^g, W_M^g, T_M^g, and B^M, $1 \leq M \leq M_{\max}$, for $M_{\max} = 191$. We plot the parameter sample S_M^g in Fig. 6(a). We observe that the parameter sample is spread throughout $\mathcal{D}$ but strongly biased towards larger values of μ_2 corresponding to a more dominant nonlinearity.

We next turn to the reduced basis approximation and construct the reduced basis space W_N^y according to the POD/Greedy sampling procedure in Sec. 3.4. To this end, we sample on Ξ_{train} with $M = M_{\max}$ and obtain $N_{\max} = 55$ for $\epsilon_{\text{tol,min}} = 1\text{E}{-}6$. We plot the parameter sample S_N^y in Fig. 6(b). We observe again that the parameter sample is biased towards larger values of μ_2 and that most samples are located on the "boundaries" of the parameter domain $\mathcal{D}$.

In Figs. 7(a) and 7(b) we plot, as a function of N and M, the maximum relative error in the energy norm $\epsilon_{N,M,\text{max,rel}}^y$ and maximum relative error bound $\Delta_{N,M,\text{max,rel}}^y$ over a test sample Ξ_{test} of size 225, respectively (see Sec. 3.5 for the

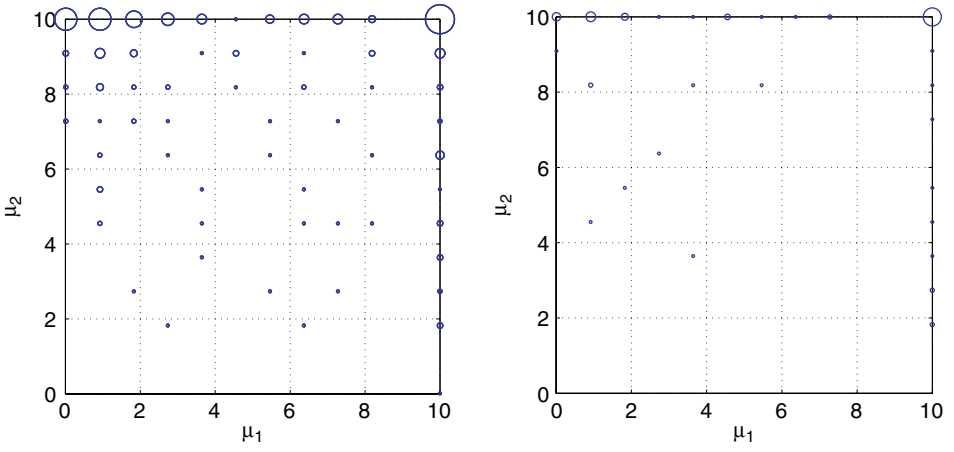

Fig. 6. Parameter samples (a) S_M^g and (b) S_N^y. The diameter of the circles scale with the frequency of the corresponding parameter in the sample.

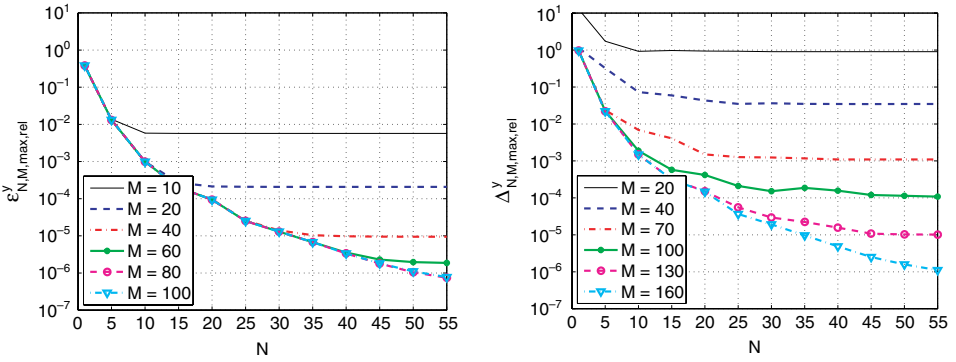

(a) (b)

Fig. 7. Convergence of the reduced basis approximation for the nonlinear model problem: (a) $\epsilon^y_{N,M,\max,\mathrm{rel}}$ and (b) $\Delta^y_{N,M,\max,\mathrm{rel}}$.

definition of these quantities). We observe very rapid convergence of the reduced basis approximation. Furthermore, the errors behave similarly as in the nonaffine example: the error levels off at smaller and smaller values as we increase M; increasing M effectively brings the error curves down. We also observe that increasing M above 80 has no (visible) effect on the convergence of the error, whereas the error bound still shows a considerable decrease up to $M = 160$. In order to obtain sharp error bounds we thus have to choose M conservatively.

In Table 7 we present, as a function of N and M, $\epsilon^y_{N,M,\max,\mathrm{rel}}$, $\Delta^y_{N,M,\max,\mathrm{rel}}$, and $\bar{\eta}^y_{N,M}$; and for the output $\epsilon^s_{N,M,\max,\mathrm{rel}}$, $\Delta^s_{N,M,\max,\mathrm{rel}}$, $\bar{\eta}^s$ (see Sec. 3.5 for the definition of these quantities). Note that the choice of (N, M) is based on the convergence of the error bound in Fig. 7(b). We observe very rapid convergence of the reduced basis (output) approximation and (output) error bound. The effectivities, $\bar{\eta}^y_{N,M}$, are greater but close to 1 throughout, we thus obtain sharp upper bounds for the true error. Due to our conservative choice of M the error contribution due to the function approximation is much smaller than the reduced basis contribution and we therefore do not obtain effectivities smaller than 1. The output effectivities are considerably larger but still acceptable, thanks to the fast convergence of the reduced basis approximation — for only $N = 20$ and $M = 100$ the relative output error bound is less than 1%.

In Table 8 we present, as a function of N and M, the online computational times to calculate $s^k_{N,M}(\mu)$ and $\Delta^{sk}_{N,M}(\mu)$ for $1 \le k \le K$. The values are normalized with respect to the computational time for the direct calculation of the truth approximation output $s^k(\mu) = \ell(y^k(\mu)), 1 \le k \le K$. The computational savings are considerable despite the output effectivities of $O(100)$: for an accuracy of less than 1% in the output bound ($N = 20$, $M = 100$) the reduction in online time is approximately a factor of 3600. We note that in the nonlinear case — as opposed to the nonaffine LTI and LTV case — the computational time to evaluate the output

Table 7. Convergence rate and effectivities as a function of N and M for the nonlinear problem.

N	M	$\epsilon^y_{N,M,\max,\mathrm{rel}}$	$\Delta^y_{N,M,\max,\mathrm{rel}}$	$\bar{\eta}^y_{N,M}$	$\epsilon^s_{N,M,\max,\mathrm{rel}}$	$\Delta^s_{N,M,\max,\mathrm{rel}}$	$\bar{\eta}^s_{N,M}$
1	40	3.83E−01	1.15E + 00	2.44	9.99E−01	2.49E + 01	14.1
5	60	1.32E−02	4.59E−02	2.43	5.35E−03	1.00E + 00	130
10	80	9.90E−04	3.41E−03	2.10	2.57E−04	7.42E−02	146
20	100	9.40E−05	4.16E−04	2.77	1.43E−05	9.06E−03	436
30	120	1.30E−05	7.34E−05	2.48	5.34E−06	1.60E−03	307
40	140	3.36E−06	8.75E−06	1.64	2.85E−06	1.90E−04	205

Table 8. Online computational times (normalized with respect to the time to solve for $s^k(\mu), 1 \leq k \leq K$) for the nonlinear problem.

N	M	$s_{N,M}(\mu, t^k), \forall\, k \in \mathbb{K}$	$\Delta^s_{N,M}(\mu, t^k), \forall\, k \in \mathbb{K}$	$s(\mu, t^k), \forall\, k \in \mathbb{K}$
1	40	5.42E−05	9.29E−05	1
5	60	9.67E−05	8.58E−05	1
10	80	1.19E−04	9.37E−05	1
20	100	1.71E−04	1.05E−04	1
30	120	2.42E−04	1.18E−04	1
40	140	3.15E−04	1.35E−04	1

bound is of the same order of magnitude as the computational time to evaluate the output approximation. This is directly related to the online computational cost: the cost to evaluate the error bound in the nonaffine LTV case is $O(KM^2N^2)$ (and $O(M^2N^2 + KN^2)$ in the LTI case), whereas the cost to evaluate the error bound in the nonlinear case is only $O(K(N + M)^2)$.

5. Conclusions

We have presented *a posteriori* error bounds for reduced basis approximations of nonaffine and certain classes of nonlinear parabolic partial differential equations. We employed the Empirical Interpolation Method to construct affine coefficient-function approximations of the nonaffine and nonlinear parametrized functions, thus permitting an efficient offline–online computational procedure for the calculation of the reduced basis approximation and the associated error bounds. The error bounds take both error contributions — the error introduced by the reduced basis approximation *and* the error induced by the coefficient function interpolation — explicitly into account and are rigorous upper bounds under certain conditions on the function approximation. The POD/Greedy sampling procedure is commonly used to generate the reduced basis space for time-dependent problems. Here, we extended these ideas to the Empirical Interpolation Method and introduced a new sampling approach to construct the collateral reduced basis space for time-varying and nonlinear functions. The new sampling approach is more efficient than our previous approach and thus also allows to consider higher parameter dimensions.

We presented numerical results that showed the very fast convergence of the reduced basis approximations and associated error bounds. We note that there

exists an optimal, i.e. most online-efficient, choice of N versus M where neither error contribution limits the convergence of the reduced basis approximation. Although our results showed that we can obtain upper bounds for the error with a judicious choice of N and M, our error bounds are, unfortunately, provably rigorous only under a very restrictive condition on the function interpolation. In the nonaffine case we can lift this restriction by replacing our current bound for the interpolation error with a new rigorous bound proposed in a recent note.[11] In the nonlinear case, however, the new bound is not applicable and the restriction remains. Rigorous bounds for nonlinear problems are the topic of current research.

Our results also showed that the computational savings to calculate the output estimate and bound in the online stage compared to direct calculation of the truth output are considerable — especially in the nonlinear case where we obtained a speed-up of $O(10^3)$. We recall that the online computational cost to evaluate the error bounds is $O(KM^2N^2)$ for the LTV problem and $O(K(M^2 + N^2))$ for the nonlinear problem considered in this paper. Moderate values of M and/or N are thus crucial for the computational efficiency of the proposed method. Recently, *hp* techniques have been proposed for reduced basis approximations[12,13] and also for the EIM.[14] These ideas help limit the online cost by reducing the size of N and M required to achieve a desired accuracy at the expense of a higher offline cost. Combining the *hp* reduced basis and EIM ideas into a unified approach would result in a further significant speed-up and is currently under investigation.

Appendix A. Computational Procedure: *A Posteriori* Error Bounds

We summarize the development of offline–online computational procedures for the calculation of $\Delta^{y,k}_{N,M}(\mu)$. We first note from standard duality arguments that

$$\begin{aligned}\varepsilon^k_{N,M}(\mu) &\equiv \sup_{v\in X} \frac{R^k(v;\mu)}{\|v\|_X} \\ &= \|\hat{e}^k(\mu)\|_X, \end{aligned} \tag{A.1}$$

where $\hat{e}^k(\mu) \in X$ is given by $(\hat{e}^k(\mu), v)_X = R^k(v;\mu), \forall\, v \in X, \forall\, k \in \mathbb{K}$; effectively a Poisson problem for each $t^k \in \mathbb{I}$. From (3.22), (3.1) and (2.7) it thus follows that $\hat{e}^k(\mu)$ satisfies

$$\begin{aligned}(\hat{e}^k(\mu), v)_X = &\sum_{m=1}^{M} \varphi^k_{Mm}(\mu) f(v;q_m) u(t^k) \\ &- \sum_{n=1}^{N} \left\{ \frac{1}{\Delta t}(y^k_{N,Mn}(\mu) - y^{k-1}_{N,Mn}(\mu)) m(\zeta_n, v) + y^k_{N,Mn}(\mu) a_0(\zeta_n, v) \right. \\ &\left. + \sum_{m=1}^{M} \varphi^k_{Mm}(\mu) y^k_{N,Mn}(\mu) a_1(\zeta_n, v, q_m) \right\}, \ \ \forall\, v \in X. \end{aligned} \tag{A.2}$$

It is clear from linear superposition that we can express $\hat{e}^k(\mu)$ as

$$\begin{aligned}\hat{e}^k(\mu) = &\sum_{m=1}^{M} \varphi_{Mm}^k(\mu) u(t^k) \mathcal{F}_m \\ &- \sum_{n=1}^{N} \left\{ \frac{1}{\Delta t}(y_{N,Mn}^k(\mu) - y_{N,Mn}^{k-1}(\mu)) \mathcal{M}_n \right. \\ &\left. + \left(\mathcal{A}_n^0 + \sum_{m=1}^{M} \varphi_{Mm}^k(\mu) \mathcal{A}_{m,n}^1 \right) y_{N,Mn}^k(\mu) \right\}, \end{aligned} \tag{A.3}$$

where we calculate $\mathcal{F}_m \in X$, $\mathcal{A}_n^0 \in X$, $\mathcal{A}_{m,n}^1 \in X$, and $\mathcal{M}_n \in X$ from

$$\begin{aligned} (\mathcal{F}_m, v)_X &= f(v; q_m), && \forall\, v \in X,\ 1 \le m \le M_{\max}, \\ (\mathcal{A}_n^0, v)_X &= a_0(\zeta_n, v), && \forall\, v \in X,\ 1 \le n \le N_{\max}, \\ (\mathcal{A}_{m,n}^1, v)_X &= a_1(\zeta_n, v, q_m), && \forall\, v \in X,\ 1 \le n \le N_{\max},\ 1 \le m \le M_{\max}, \\ (\mathcal{M}_n, v)_X &= m(\zeta_n, v), && \forall\, v \in X,\ 1 \le n \le N_{\max}; \end{aligned} \tag{A.4}$$

note $\mathcal{F}$, $\mathcal{A}^{0,1}$, and $\mathcal{M}$ are parameter-independent. Given these quantities, the offline–online decomposition of (A.1) directly follows from the affine case.[19]

The evaluation of $\Phi_M^{\mathrm{na},k}(\mu)$ is similar; to this end, we first calculate $\mathcal{F}_{M+1} \in X$ and $\mathcal{A}_{M+1,n}^1 \in X$ from

$$\begin{aligned} (\mathcal{F}_{M+1}, v)_X &= f(v; q_{M+1}), && \forall\, v \in X, \\ (\mathcal{A}_{M+1,n}^1, v)_X &= a_1(\zeta_n, v; q_{M+1}), && \forall\, v \in X,\ 1 \le n \le N_{\max}. \end{aligned} \tag{A.5}$$

It then follows from (3.23) and standard duality arguments that

$$\begin{aligned}\Phi_M^{\mathrm{na},k}(\mu)^2 = &\, u(t^k)^2 \Lambda_{M+1M+1}^{ff} \\ &+ \sum_{n=1}^{N} y_{N,Mn}^k(\mu) \left\{ u(t^k) \Lambda_{nM+1M+1}^{a_1 f} + \sum_{n'=1}^{N} y_{N,Mn'}^k(\mu) \Lambda_{nn'M+1M+1}^{a_1 a_1} \right\}, \end{aligned}$$

where the parameter-independent quantities Λ are defined as

$$\begin{aligned} \Lambda_{M+1M+1}^{ff} &= (\mathcal{F}_{M+1}, \mathcal{F}_{M+1})_X; \\ \Lambda_{nM+1M+1}^{a_1 f} &= -2(\mathcal{F}_{M+1}, \mathcal{A}_{M+1,n}^1)_X, \quad 1 \le n \le N_{\max}; \\ \Lambda_{nn'M+1M+1}^{a_1 a_1} &= (\mathcal{A}_{M+1,n}^1, \mathcal{A}_{M+1,n'}^1)_X, \quad 1 \le n, n' \le N_{\max}. \end{aligned} \tag{A.6}$$

The offline–online decomposition is now clear. In the offline stage we first compute the quantities $\mathcal{F}$, $\mathcal{A}^{0,1}$, and $\mathcal{M}$ from (A.4) and (A.5) and subsequently perform the necessary inner products for the evaluation of $\|\hat{e}^k(\mu)\|_X$; this requires (to leading order) $O(M_{\max} N_{\max})$ expensive "truth" finite element solutions, and

$O(M_{\max}^2 N_{\max}^2)$ $\mathcal{N}$-inner products. In the online stage — given a new parameter value μ and associated reduced basis solution $\underline{y}_{N,M}^k(\mu)$, $\forall\, k \in \mathbb{K}$ — the computational cost to evaluate $\Delta_{N,M}^{y,k}(\mu)$ and $\Delta_{N,M}^{s,k}(\mu)$, $\forall\, k \in \mathbb{K}$, is $O(KM^2N^2)$. Thus, all online calculations needed are *independent* of $\mathcal{N}$.

Acknowledgments

I would like to thank Professor A. T. Patera of MIT and Professor Y. Maday of University Paris VI for their many invaluable contributions to this work. I would also like to thank J. L. Eftang of NTNU for helpful discussions and the reviewer for helpful comments to improve the manuscript. This work was supported by the Excellence Initiative of the German federal and state governments, by DARPA and AFOSR under Grant F49620-03-1-0356, DARPA/GEAE and AFOSR under Grant F49620-03-1-0439, and the Singapore-MIT Alliance.

References

1. B. O. Almroth, P. Stern and F. A. Brogan, Automatic choice of global shape functions in structural analysis, *AIAA J.* **16** (1978) 525–528.
2. Z. J. Bai, Krylov subspace techniques for reduced-order modeling of large-scale dynamical systems, *Appl. Numer. Math.* **43** (2002) 9–44.
3. E. Balmes, Parametric families of reduced finite element models: Theory and applications, *Mech. Syst. Signal Process.* **10** (1996) 381–394.
4. M. Barrault, N. C. Nguyen, Y. Maday and A. T. Patera, An "empirical interpolation" method: Application to efficient reduced-basis discretization of partial differential equations, *C. R. Acad. Sci. Paris, Série I* **339** (2004) 667–672.
5. A. Barrett and G. Reddien, On the reduced basis method, *Z. Angew. Math. Mech.* **75** (1995) 543–549.
6. T. T. Bui, M. Damodaran and K. Wilcox, Proper orthogonal decomposition extensions for parametric applications in transonic aerodynamics (AIAA Paper 2003–4213), in *Proc. of the 15th AIAA Computational Fluid Dynamics Conference*, June 2003.
7. C. Canuto, T. Tonn and K. Urban, *A posteriori* error analysis of the reduced basis method for nonaffine parametrized nonlinear pdes, *SIAM J. Numer. Anal.* **47** (2009) 2001–2022.
8. J. Chen and S.-M. Kang, Model-order reduction of nonlinear mems devices through arclength-based Karhunen–Loéve decomposition, in *Proc. of the IEEE Int. Symp. Circuits and Systems*, Vol. 2 (IEEE, 2001), pp. 457–460.
9. Y. Chen and J. White, A quadratic method for nonlinear model order reduction, in *Proc. of the Int. Conf. on Modeling and Simulation of Microsystems* (NST, 2000), pp. 477–480.
10. E. A. Christensen, M. Brøns and J. N. Sørensen, Evaluation of proper orthogonal decomposition-based decomposition techniques applied to parameter-dependent nonturbulent flows, *SIAM J. Scientific Computing* **21** (2000) 1419–1434.
11. J. L. Eftang, M. A. Grepl and A. T. Patera, *A posteriori* error bounds for the empirical interpolation method, *C. R. Acad. Sci. Paris, Ser. I* **348** (2010) 575–579.
12. J. L. Eftang, D. K. Knezevic and A. T. Patera, An *hp* certified reduced basis method for parametrized parabolic partial differential equations, *Math. Computer Model. Dynam. Syst.* **17** (2011) 395–422.

13. J. L. Eftang, A. T. Patera and E. M. Rønquist, An "*hp*" certified reduced basis method for parametrized elliptic partial differential equations, *SIAM J. Scientific Computing* **32** (2010) 3170–3200.
14. J. L. Eftang and B. Stamm, Parameter multi-domain "*hp*" empirical interpolation, *Int. J. Numer. Methods Engrg.*, submitted 2011.
15. J. P. Fink and W. C. Rheinboldt, On the error behavior of the reduced basis technique for nonlinear finite element approximations, *Z. Angew. Math. Mech.* **63** (1983) 21–28.
16. H. Fujita and T. Suzuki, Evolution problems, in *Handbook of Numerical Analysis*, Vol. II, eds. P. G. Ciarlet and J.-L. Lions (Elsevier, 1991), pp. 789–928.
17. M. A. Grepl, Reduced-basis approximation and *a posteriori* error estimation for parabolic partial differential equations, Ph.D. thesis, Massachusetts Institute of Technology, 2005.
18. M. A. Grepl, Y. Maday, N. C. Nguyen and A. T. Patera, Efficient reduced-basis treatment of nonaffine and nonlinear partial differential equations, *ESAIM*: *M2AN* **41** (2007) 575–605.
19. M. A. Grepl and A. T. Patera, *A posteriori* error bounds for reduced-basis approximations of parametrized parabolic partial differential equations, *ESAIM*: *M2AN* **39** (2005) 157–181.
20. B. Haasdonk and M. Ohlberger, Reduced basis method for finite volume approximations of parametrized linear evolution equations, *ESAIM*: *M2AN* **42** (2008) 277–302.
21. D. B. P. Huynh, G. Rozza, S. Sen and A. T. Patera, A successive constraint linear optimization method for lower bounds of parametric coercivity and inf-sup stability constants, *C. R. Acad. Sci. Paris Sér. I* **345** (2007) 473–478.
22. K. Ito and S. S. Ravindran, A reduced-order method for simulation and control of fluid flows, *J. Comput. Phys.* **143** (1998) 403–425.
23. D. J. Knezevic, N. C. Nguyen and A. T. Patera, Reduced basis approximation and *a posteriori* error estimation for the parametrized unsteady Boussinesq equations, *Math. Models Methods Appl. Sci.* **21** (2011) 1415–1442.
24. D. J. Knezevic and A. T. Patera, A certified reduced basis method for the Fokker–Planck equation of dilute polymeric fluids: FENE dumbbells in extensional flow, *SIAM J. Scientific Computing* **32** (2010) 793–817.
25. S. Lall, J. E. Marsden and S. Glavaski, A subspace approach to balanced truncation for model reduction of nonlinear control systems, *Int. J. Robust Nonlinear Control* **12** (2002) 519–535.
26. J. L. Lions, *Quelques Méthodes de Résolution des Problèmes aux Limites Non-Linéaires* (Dunod, 1969).
27. L. Machiels, Y. Maday, I. B. Oliveira, A. T. Patera and D. V. Rovas, Output bounds for reduced-basis approximations of symmetric positive definite eigenvalue problems, *C. R. Acad. Sci. Paris, Sér. I* **331** (2000) 153–158.
28. Y. Maday, N. C. Nguyen, A. T. Patera and S. H. Pau, A general multipurpose interpolation procedure: The magic points, *Commun. Pure Appl. Anal.* **8** (2009) 383–404.
29. M. Meyer and H. G. Matthies, Efficient model reduction in non-linear dynamics using the Karhunen–Loève expansion and dual-weighted-residual methods, *Comput. Mech.* **31** (2003) 179–191.
30. N. C. Nguyen, K. Veroy and A. T. Patera, Certified real-time solution of parametrized partial differential equations, in *Handbook of Materials Modeling*, ed. S. Yip (Springer, 2005), pp. 1523–1558.

31. N. C. Nguyen, *A posteriori* error estimation and basis adaptivity for reduced-basis approximation of nonaffine-parametrized linear elliptic partial differential equations, *J. Comput. Phys.* **227** (2007) 983–1006.
32. N. C. Nguyen, G. Rozza and A. T. Patera, Reduced basis approximation and *a posteriori* error estimation for the time-dependent viscous Burgers' equation, *Calcolo* **46** (2009) 157–185.
33. A. K. Noor and J. M. Peters, Reduced basis technique for nonlinear analysis of structures, *AIAA J.* **18** (1980) 455–462.
34. J. R. Phillips, Projection-based approaches for model reduction of weakly nonlinear systems, time-varying systems, in *IEEE Transactions On Computer-Aided Design of Integrated Circuit and Systems*, Vol. 22 (2003), pp. 171–187 .
35. T. A. Porsching, Estimation of the error in the reduced basis method solution of nonlinear equations, *Mathematics of Computation* **45** (1985) 487–496.
36. C. Prud'homme, D. Rovas, K. Veroy, Y. Maday, A. T. Patera and G. Turinici, Reliable real-time solution of parametrized partial differential equations: Reduced-basis output bound methods, *Journal of Fluids Engineering* **124** (2002) 70–80.
37. A. Quarteroni, R. Sacco and F. Saleri, *Numerical Mathematics*, Texts in Applied Mathematics, Vol. 37 (Springer, 1991).
38. A. Quarteroni and A. Valli, *Numerical Approximation of Partial Differential Equations*, 2nd edn. (Springer, 1997).
39. M. Rewienski and J. White, A trajectory piecewise-linear approach to model order reduction and fast simulation of nonlinear circuits and micromachined devices, in *IEEE Trans. Computer-Aided Design of Integrated Circuit Syst.* **22** (2003) 155–170.
40. W. C. Rheinboldt, On the theory and error estimation of the reduced basis method for multi-parameter problems, *Nonlinear Analysis, Theory, Methods and Applications* **21** (1993) 849–858.
41. D. V. Rovas, L. Machiels and Y. Maday, Reduced-basis output bound methods for parabolic problems, *IMA Journal of Numerical Analysis* **26** (2006) 423–445.
42. G. Rozza, D. B. P. Huynh and A. T. Patera, Reduced basis approximation and *a posteriori* error estimation of affinely parametrized elliptic coercive partial differential equations, *Archives of Computational Methods in Engineering* **15** (2008) 229–275.
43. J. M. A. Scherpen, Balancing for nonlinear systems, *Systems and Control Letters* **21** (1993) 143–153.
44. L. Sirovich, Turbulence and the dynamics of coherent structures, part 1: Coherent structures, *Quarterly of Applied Mathematics* **45** (1987) 561–571.
45. V. Thomeé, *Galerkin Finite Element Methods for Parabolic Problems*, Springer Series in Computational Mathematics (Springer-Verlag, 2006).
46. K. Veroy and A. T. Patera, Certified real-time solution of the parametrized steady incompressible Navier-Stokes equations; Rigorous reduced-basis *a posteriori* error bounds, *International Journal for Numerical Methods in Fluids* **47** (2005) 773–788.
47. K. Veroy, C. Prud'homme and A. T. Patera, Reduced-basis approximation of the viscous Burgers equation: Rigorous *a posteriori* error bounds, *C. R. Acad. Sci. Paris, Sér. I* **337** (2003) 619–624.
48. K. Veroy, C. Prud'homme, D. V. Rovas and A. T. Patera, *A posteriori* error bounds for reduced-basis approximation of parametrized noncoercive and nonlinear elliptic partial differential equations (AIAA Paper 2003–3847), in *Proc. of the 16th AIAA Computational Fluid Dynamics Conference*, June 2003.
49. K. Veroy, D. Rovas and A. T. Patera, *A posteriori* error estimation for reduced-basis approximation of parametrized elliptic coercive partial differential equations:

"Convex inverse" bound conditioners, *Control, Optimisation and Calculus of Variations* **8** (2002) 1007–1028. Special Volume: A tribute to J.-L. Lions.
50. D. S. Weile, E. Michielssen and K. Gallivan, Reduced-order modeling of multiscreen frequency-selective surfaces using Krylov-based rational interpolation, *IEEE Transactions on Antennas and Propagation* **49** (2001) 801–813.